



HAL
open science

Molecularly imprinted polymers for per-and polyfluoroalkyl substances enrichment and detection

Aicha Tasfaout, Farah Ibrahim, Aoife Morrin, Hugues Brisset, Ilaria Sorrentino, Clément Nanteuil, Guillaume Laffite, Ian Nicholls, Fiona Regan, Catherine Branger

► To cite this version:

Aicha Tasfaout, Farah Ibrahim, Aoife Morrin, Hugues Brisset, Ilaria Sorrentino, et al.. Molecularly imprinted polymers for per-and polyfluoroalkyl substances enrichment and detection. *Talanta*, 2023, 258, pp.124434. 10.1016/j.talanta.2023.124434 . hal-04475513

HAL Id: hal-04475513

<https://univ-tln.hal.science/hal-04475513>

Submitted on 23 Feb 2024

HAL is a multi-disciplinary open access archive for the deposit and dissemination of scientific research documents, whether they are published or not. The documents may come from teaching and research institutions in France or abroad, or from public or private research centers.

L'archive ouverte pluridisciplinaire **HAL**, est destinée au dépôt et à la diffusion de documents scientifiques de niveau recherche, publiés ou non, émanant des établissements d'enseignement et de recherche français ou étrangers, des laboratoires publics ou privés.

Molecularly imprinted polymers for per- and polyfluoroalkyl substances enrichment and detection

Aicha Tasfaout^{1#}, Farah Ibrahim^{2#}, Aoife Morrin¹, Hugues Brisset², Ilaria Sorrentino³, Clément Nanteuil³, Guillaume Laffite³, Ian A. Nicholls⁴, Fiona Regan¹, Catherine Branger^{2,*}

¹ School of Chemical Sciences, National Centre for Sensor Research, Dublin City University, Glasnevin, Dublin 9, Ireland

² Université de Toulon, Laboratoire Matériaux Polymères Interfaces Environnement Marin (MAPIEM), Toulon, France

³ Klearia, 61 Avenue Simone Veil, CEEI Nice Côte d'Azur - Immeuble Premium, 06200 Nice, France

⁴ Bioorganic & Biophysical Chemistry Laboratory, Department of Chemistry & Biomedical Sciences, Linnaeus University, SE-39182 Kalmar, Sweden.

Authors with equal contribution

Corresponding author: branger@univ-tln.fr

Abstract

Per- and polyfluoroalkyl substances (PFAS) are highly toxic pollutants of significant concern as they are being detected in water, air, fish and soil. They are extremely persistent and accumulate in plant and animal tissues. Traditional methods of detection and removal of these substances use specialised instrumentation and require a trained technical resource for operation. Molecularly imprinted polymers (MIPs), polymeric materials with predetermined selectivity for a target molecule, have recently begun to be exploited in technologies for the selective removal and monitoring of PFAS in environmental waters. This review offers a comprehensive overview of recent developments in MIPs, both as adsorbents for PFAS removal and sensors that selectively detect PFAS at environmentally-relevant concentrations. PFAS-MIP adsorbents are classified according to their method of preparation (e.g., bulk or precipitation polymerization, surface imprinting), while PFAS-MIP sensing materials are described and discussed according to the transduction methods used (e.g., electrochemical, optical). This review aims to comprehensively discuss the PFAS-MIP research field. The efficacy and challenges facing the different applications of these materials in environmental water applications are discussed, as well as a perspective on challenges for this field that need to be overcome before exploitation of the technology can be fully realised.

Keywords Per- and polyfluoroalkyl substances (PFAS), molecularly imprinted polymers (MIPs), sensor, adsorption, environmental waters

Contents

1. Introduction.....	3
2. MIPs as selective adsorbents for PFAS.....	6
2.1.Preparation of adsorbents	7
2.2.Performance of the adsorbents	10
3. MIPs as selective sensing materials for PFAS.....	18
3.1.Electrochemical sensors	18
3.2.Photoelectrochemical sensors	22
3.3.Electrochemiluminescent sensors	23
3.4.Photoluminescent sensors.....	23
3.5.Surface plasmon resonance (and optical intensity-based sensors)	26
4. Conclusions.....	26

Abbreviations

AA	Acrylic acid	FTO	Fluorine-doped tin oxide
AAM	Acrylamide	FTS	Fluorotelomer sulfonate
An	Aniline	GC	Gas chromatography
APTES	Aminopropyltriethoxysilane	GAC	Granular activated carbon
BPA	Bisphenol A	GCE	Glassy carbon electrode
CMS	Carbon microspheres	HPLC	High performance liquid chromatography
CQD	Carbon quantum dots	IF	Imprinting factor
CTAB	Cetyltrimethylammonium bromide	LC	Liquid chromatography
DBP	Dibutyl phthalate	LC-MS	Liquid chromatography coupled with mass spectroscopy
2,4-D	2,4-Dichlorophenoxyacetic acid	LOD	Limit of detection
ECH	Epichlorohydrin	MAA	Methacrylic acid
ECL	Electrochemiluminescence	MBA	N,N'-Methylenebis(acrylamide)
EGDMA	Ethylene glycol dimethylacrylate	MIP	Molecularly imprinted polymer
FITC	Fluorescein 6-isothiocyanate	MMIP	Magnetic molecularly imprinted polymers

MS	Mass spectrometry	PFOS	Perfluorosulfonic acid
MS/MS	Tandem mass spectrometry	PFOSF	Perfluorooctanesulfonyl fluoride
MSN	Mesoporous silica nanoparticles	PFPeA	Perfluoropentanoic acid
MTAC	Methacryloyloxyethyl trimethyl ammonium chloride	PFTeDA	Perfluorotetradecanoic acid
		PFUnA	Perfluoroundecanoic acid
MWCNT	Multi-walled carbon nanotubes	PL	Photoluminescence
NIP	Non-imprinted polymer	PLMIP	Photoluminescent molecularly imprinted polymer
NP	Nanoparticle	POF	Plastic optical fiber
NTA	Nanotube arrays	PPy	Poly-pyrrole
NF	Nanoflake (arrays)	Py	Pyrrole
PANI	Polyaniline	QD	Quantum dots
PCP	Phencyclidine	RSD	Relative standard deviation
oPD	o-Phenyldiamine	SDBS	Sodium dodecylbenzene sulfonate
PEC	Photoelectrochemical	SDS	Sodium dodecyl sulfate
PFAS	Per- and polyfluoroalkyl substances	SPE	Screen-printed electrode or Solid phase extraction
PFBA	Perfluorobutanoic acid	SPR	Surface plasmon resonance
PFBS	Perfluorobutanesulfonic acid	TEOS	Tetraethoxysilane
PFC	Per- and polyfluoroalkyl compounds	TFMAA	2-(Trifluoromethyl) acrylic acid
PFDA	Perfluorodecanoic acid	TRIA	Trimethylolpropane triacrylate
PFDoA	Perfluorododecanoic acid	TRIM	Trimethylolpropane trimethacrylate
PFHxA	Perfluorohexanoic acid	UHPLC	Ultra-high performance liquid chromatography
PFHpA	Perfluoroheptanoic acid	VBT	(4Vinylbenzyl)thymine
PFHSK	Perfluorohexanesulfonic acid potassium salt	VPy	Vinylpyridine
PFNA	Perfluorononanoic acid	WHO	World health organization
PFOA	Perfluorooctanoic acid		

33 **1. Introduction**

34 Per- and polyfluorinated alkyl substances (PFAS), also known as per- and polyfluorinated compounds
35 (PFC), have been used for decades in a range of applications like firefighting foams, non-stick cookware

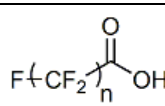
36 and water and stain-resistant clothing [1,2]. They make up a large group of over 4700 artificial chemicals, to
 37 which humans are exposed daily, in soil, water and air, and are of significant health concern.
 38 Epidemiological studies show that PFAS constitute a danger to the endocrine and reproductive systems [1].

39 The PFAS class of compounds covers fully (per-) or partly (poly-) fluorinated aliphatic compounds in
 40 which at least one carbon atom is fully fluorinated. The general structure of the perfluorinated aliphatic
 41 compounds contain the moiety $C_nF_{2n+1}-R$, where n is the number of carbon atoms, while R refers to the
 42 functional group (carboxylate, sulfonate, phosphonate...etc.) [3]. Amongst PFAS, perfluorooctane sulfonate
 43 (PFOS) and perfluorooctanoic acid (PFOA) (Table 1) have drawn particular attention and generated
 44 regulatory concerns in recent years. These are the most frequently detected PFASs in the environment [4,5].
 45 They are highly resistant to thermal, biological and chemical decomposition and photolysis and thus highly
 46 persistent [6,7]. They have been listed as persistent organic pollutants by the Stockholm Convention and in
 47 the reduction plan by the US Environment Protection Agency [8,9]. The World Health Organization
 48 (WHO) has recently set maximal values of $0.4 \mu\text{g}\cdot\text{L}^{-1}$ and $4 \mu\text{g}\cdot\text{L}^{-1}$ for PFOS and PFOA respectively in
 49 drinking water intended for human consumption [10].

50 The C-F bond is highly polar and one of the strongest covalent bonds ($544 \text{ kJ}\cdot\text{mol}^{-1}$), which renders this
 51 class of chemical highly resistant to complete degradation [11]. Moreover, the low polarizability of the
 52 fluorine atom imparts hydrophobic and lipophobic properties, while the terminal functional R group gives
 53 them chemical and thermal stability [12]. Additionally, most PFAS containing long per-fluorinated chains
 54 exhibit amphiphilic properties, owing to the hydrophobic tail and the hydrophilic functional group. This
 55 contributes to their high solubility in water and absorption in soil, which paired with their high stability and
 56 resistance to degradation, leads to severe risks of pollution of natural resources and persistence in these
 57 environments [13]. Furthermore, PFAS are most likely to be absorbed by the human body through oral
 58 ingestion, as they persist in drinking water, transferred to food through non-stick cookware and certain
 59 cleaning products, and sometimes even found in food packaging [1,2].

60

61 **Table 1.** Name, chemical structure and acronym of several PFASs, including PFOS and PFOA ($n = 8$).

Name	Structure	Acronym
Perfluoroalkyl carboxylic acid (PFCA)		n = 4, PFBA; n = 5, PFPA; n = 6, PFHxA; n = 7, PFHpA; n = 8, PFOA; n = 9, PFNA; n = 10, PFDA;

		n = 11, PFUnA; n = 12, PFDoA
Perfluoroalkyl sulfonic acid (PFSA)	$\text{F}-(\text{CF}_2)_n-\text{S}(=\text{O})_2\text{OH}$	n = 4, PFBS; n = 5, PFPS; n = 6, PFHxS; n = 7, PFHpS; n = 8, PFOS
Perfluoroalkyl phosphonic acid (PFPA)	$\text{F}-(\text{CF}_2)_n-\text{P}(=\text{O})(\text{OH})_2$	n = 6, PFHxPA; n = 8, PFOPA; n = 10, PFDPA
Perfluoroalkane sulphonamide (PFASA)	$\text{F}-(\text{CF}_2)_n-\text{S}(=\text{O})_2\text{NH}_2$	n = 4, FBASA; n = 6, FHxSA; n = 8, FOASA

62

63 PFAS consequences on human health have been getting considerable attention [14]. Toxicological studies
64 usually tend to focus on PFOS and PFOA given their extensive use in various industries in the past and
65 present. PFAS have been classified as endocrine disruptors, as animal studies showed that they may alter
66 cholesterol metabolism and thyroid levels leading to severe conditions in humans [1,2,15]. More recent
67 studies investigate the relationship between exposure to PFAS in general and abnormal ovarian functions,
68 decline in fertility and risks of cancer in the reproductive system [1,15], although there is not enough
69 evidence to confirm a causal relationship. In addition, some toxicological studies have shown that long-
70 chain perfluoroalkyl acids might behave additively or interact synergistically or antagonistically when found
71 in mixtures depending on the compounds in question, their dose levels, and ratios in the mixture [14].

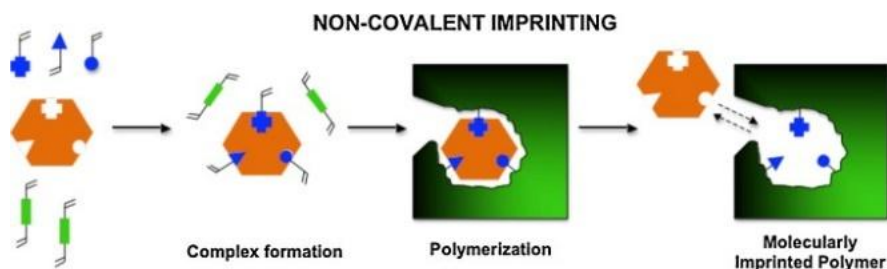
72 Therefore, there have been many efforts to analyse these emerging contaminants in the environment,
73 especially for drinking water and the food industry. Traditional methods used for the detection of PFAS are
74 liquid chromatography (LC) and gas chromatography (GC) coupled with either mass spectrometry (MS) or
75 tandem mass spectrometry (MS/MS). However, these commonly used techniques usually require a pre-
76 treatment step based on liquid-liquid extraction or solid phase extraction (SPE). Moreover, they have some
77 inherent disadvantages and limitations that can limit their use for the monitoring of PFAS: for example the
78 cost, the usage of large amounts of solvent, the risk of contamination in the different steps and the
79 interference of other compounds present in complex media that could falsify the results. Molecularly
80 Imprinted Polymers (MIPs) appear to be an attractive alternative to overcome these shortcomings. Indeed,
81 they can be used as selective absorbents for an efficient sample processing or as recognition elements in the

82 design of chemical sensors. MIPs in general represent highly selective receptor materials and are designed to
83 bind a specific analyte through specific imprints, which can be used either as recognition element in sensors
84 or for molecular separations by selective sorption [16].

85 The MIP synthesis technique consists of co-polymerising one or multiple functional monomers and a cross-
86 linker around a template which is the target of interest (Figure 1). Once the template is removed, vacant
87 imprinted binding cavities are generated that retain the conformation, the complementary functionality, and
88 the size of the template. Therefore, MIPs exhibit strong affinity and high specificity for the target molecules,
89 compared to their non-imprinted homologues (NIPs) which omit the template molecule during
90 polymerization. The non-covalent approach is the most widespread across research published about MIP
91 systems thanks to its simplicity and the convenience of using readily available functional monomers. In this
92 technique, the target molecule interacts with the monomers through interactions including hydrogen
93 bonding, van der Waals forces, $\pi-\pi$ interactions, and/or hydrophobic or ionic bonds. Hence, the selection
94 of suitable monomers able to evolve good and stable interactions with the template is a crucial step in this
95 approach in order to achieve a successful imprinting of the target [17].

96 Furthermore, the most common kind of MIPs reported in the literature are highly cross-linked polymers.
97 They benefit from inherently high mechanical stability and robustness in a wide range of temperatures, pHs
98 and solvents and can be prepared in varying types of formats and supports [18,19]. As a result, MIPs are
99 extensively used in many environmental applications such as selective adsorbents for sample pretreatment
100 [20], sensors for the selective detection of the target analyte [21] and catalysis [22]. In this review, the role,
101 and the applications of MIPs in the enrichment and detection of PFAS in varied environmental
102 matrices~~water~~ are investigated across the recently published literature, as they remain a relatively new
103 technology in this field.

104



105

106 *Fig. 1. Schematic representation of the synthesis of a MIP (Adapted from [23], Reprinted-with permission from*
107 *Elsevier, Copyright 2012).*

108

109 **2. MIPs as selective adsorbents for PFAS**

110 Various adsorbents such as granular activated carbon (GAC), powder activated carbon (PAC), resins, ion
111 exchange polymers, alumina, boehmite and clay minerals have been used in order to extract and to detect

112 PFAS [24–26]. However, these materials have no selectivity for PFAS and in complex media several other
113 compounds can be extracted as well which lowers the adsorption efficiency and distorts the results.
114 Molecularly imprinted polymers appear to be an attractive material to allow selective extraction of PFAS.

115 *2.1. Preparation of adsorbents*

116 Table 2 lists the MIPs prepared for use as adsorbents for PFAS, specifying their compositions, preparation
117 methods and performances. As far as MIPs are expected to be used as adsorbents, the desired format is
118 usually that of particles. This format can be obtained directly through precipitation polymerization or surface
119 imprinting technology. Bulk polymerization is easier to implement but requires the grinding and sieving of
120 the MIPs to obtain non-monolithic polymers. For example, Deng and co-workers investigated PFOS-MIP
121 adsorbents that were synthesized by bulk copolymerization of 4-vinylpyridine (4-VPy) as functional
122 monomer with either trimethylolpropane triacrylate (TRIA) or ethyleneglycol dimethacryate (EGDMA) as
123 cross-linkers in presence of PFOA or PFOS as templates [27]. Different molar ratios of
124 PFOA/monomer/cross-linker were tested and it was noticed that the adsorbent prepared using PFOA as a
125 template showed the highest sorption capacity. This was potentially attributed to the higher water solubility
126 of PFOA than that of PFOS as well as the electrostatic interaction in the low pH conditions used for the
127 sorption experiments. Cao and co-workers prepared MIP particles for PFOA by precipitation
128 polymerization [28]. They optimized the nature of the functional monomer by using several commercial
129 monomers that are commonly used for MIP synthesis, including acrylic acid (AA), acrylamide (AAM), 2-
130 VPy and 4-VPy. They included 2-(trifluoromethyl) acrylic acid (TFMAA) in their study to provide
131 additional fluorine-fluorine interaction between the functional monomer and the template. Among all tested
132 monomers, AAM gave the MIP with the highest adsorption capacity, possibly because of the hydrogen
133 bonding between the amide group of AAM and the carboxylic acid group of PFOA. Cao and co-workers
134 further used TFMAA and 4-VPy as binary functional monomers and PFOA as template for preparing MIPs
135 for PFOA and PFOS removal by precipitation polymerization (Figure 2) [29]. The presence of TFMAA in
136 addition to AAM in the binary functional monomer MIPs enhanced their adsorption capacities compared to
137 AAM based-MIPs due to the additional fluorine–fluorine interactions provided [28].

138 In another approach, Yu and co-workers used chitosan to prepare MIP adsorbents for the selective removal
139 of PFOS from aqueous solutions [30]. Chitosan is a linear natural polymer that these authors cross-linked
140 with epichlorohydrin (ECH) in a two-step procedure. During the second step, which corresponds to the MIP
141 preparation, the effect of the pH of the solution was studied. It was found that the optimal MIP adsorbents
142 were imprinted in PFOS solution at pH 3 where the electrostatic attraction between the sulfonic group in
143 PFOS and the protonated amino groups in the chitosan molecules is favoured.

144 In an original approach, Yan and co-workers prepared two molecularly imprinted phenolic resin
145 adsorbents for dispersive solid-phase extraction using a portable syringe filter [31,32]. The device
146 was combined with LC-MS/MS. An analytical method was established for the rapid and
147 selective extraction and determination of long-chain PFCs in food samples (milk and pork).
148 PFNA or perfluorotetradecanoic acid (PFTeDA) were used as templates, phenolic compounds as
149 monomers, glutaraldehyde as cross-linking agent and polyethylene glycol-6000 as the porogen.

150 The surface imprinting technique was developed to enhance the mass transfer rate and increase the
151 accessibility of the recognition sites [33]. For that purpose, the surface of particles (usually inorganic in
152 nature) is covered with an imprinted layer to provide core-shell type particles. Several kinds of particles
153 were investigated to prepare MIP adsorbents for PFASs. Du and co-workers employed mesoporous silica
154 nanoparticles (MSNs) as carriers to prepare core-shell structural MSNs/MIPs to separate and enrich PFOS
155 in water samples [34]. Cao and co-workers prepared surface imprinted MIPs using multi-walled carbon
156 nanotubes (MWCNTs) as supporting materials [35]. MWCNTs were selected due to their interesting
157 properties such as their large surface area, their highly porous and hollow structure, their high density of π -
158 electrons, and their ease of chemical modification. They used PFOA as template and AAM as functional
159 monomer and reproduced the same protocol used to prepare their conventional AAM based-MIP
160 previously described [28].

161 The development of magnetic molecularly imprinted polymers (MMIPs) to remove PFOS has attracted
162 attention from Du and co-workers since they can provide superparamagnetic materials [36]. Indeed, these
163 superparamagnetic nanoparticles can be easily separated and thus, the target molecules can be extracted
164 rapidly. In this context, they synthesized MMIPs using PFOS as a template molecule on the surface of
165 functionalized Fe_2O_3 nanoparticles (Figure 3) [36].

166 In the same perspective, Lin *et al.* constructed a superparamagnetic core-shell MIP via self-
167 polymerization of dopamine around PFOS and immobilization onto Fe_3O_4 substrate [37]. The
168 same group designed a MIP adsorbent by surface imprinting on carbon microspheres (CMSs) as carrier
169 [38]. CMSs were chosen because they are stable in acidic conditions and their mechanical stability is also
170 good. An amine group was introduced onto the surface of the CMSs by silanization to increase the reactivity
171 of the surface. They used PFOA as template and methacryloyloxyethyl trimethyl ammonium chloride
172 (MTAC) and TFMAA as binary functional monomers to include two different kinds of binding forces,
173 which provided good binding selectivity to the template. The tertiary amine groups of the MTAC monomer
174 and the carboxyl groups in the TFMAA can be easily protonated at low pH. Hence, the electrostatic
175 interaction between the functional monomers and the PFOS played an important role in the adsorption
176 process at acidic pH as well as the fluorine-fluorine interaction most probably involved in the adsorption.

177 Hu and co-workers were concerned by the destruction of harmful perfluorinated pollutants during the
178 regeneration process of the MIPs adsorbents [39]. They combined the MIP adsorption for PFASs with TiO_2
179 photocatalysis in order to develop a photocatalyst to achieve selective removal of perfluorinated compounds
180 from secondary effluents and simultaneous regeneration the polymers. The photocatalyst was prepared by
181 surface coating of vinyl-functionalized TiO_2 nanotube arrays (NTAs) with a thin MIP layer using
182 methacrylic acid (MAA) and trimethylpropane trimethacrylate (TRIM) as functional monomer and cross-
183 linker respectively. Wu and co-workers fabricated a similar MIP-modified TiO_2 photocatalyst using AAM
184 and EGDMA as monomers [40].

185 In all studies reported, subsequent to MIP synthesis, the removal of the template and unreacted monomers
186 was achieved by successive extraction using an organic solvent or a mixture of an organic solvent with an

187 acid or a base or pure water until no template was detected in the eluate. Therefore, no contamination with
188 PFAS template to the environment is assumed during MIP usage.

189 ***2.2. Properties/characteristics of the adsorbents***

190 PFOS and PFOA adsorption on MIPs are pH dependent. Indeed, the pH of the solution not only influences
191 the properties of the adsorbent surface but also affects the speciation of target pollutant in solution. For
192 example, PFOA ionizes in water to form a perfluorocarboxylic anion when the solution pH is above its pKa
193 value of 2.8 [41] whereas the pKa of the sulfonic group in PFOS is about -3.27 [42]. In most cases, MIPs
194 show highest removal rates for PFOS and PFOA at low pH where the functional groups present in the
195 adsorbents such as pyridine [27,29], amine [30,36] and quaternary ammonium [38] are positively charged.
196 Consequently, electrostatic attraction between the target and the MIP adsorbent dominates the adsorption
197 process. With increasing solution pH, deprotonated forms of the functional groups are sometimes formed
198 and electrostatic repulsion between the target and the MIP adsorbate becomes stronger, reducing the binding
199 affinity and decreasing the adsorption capacity [28,29,35,38].

200 Langmuir and Freundlich models have been used to describe the binding characteristics of the MIP
201 adsorbents prepared for PFAS extraction. The Langmuir model assumes that binding sites present on the
202 adsorbent surface are identical and that adsorption is mainly monolayer, whereas the Freundlich model
203 assumes binding sites are different and adsorption is multilayer on a heterogeneous surface. The adsorption
204 isotherms of several PFAS MIPs revealed that the Langmuir model describes the adsorption behavior of
205 PFAS on reported MIPs adsorbents well [28,29,35,36,38], while for others the Freundlich model seems to
206 provide a better fit to the experimental results [34,39,40] (Table 2).

207 Since the knowledge of the adsorption kinetics between analyte and adsorbent is an important feature for
208 extraction applications, it has been studied by most authors who prepared MIPs for PFAS. The two kinetics
209 models used for describing PFASs binding are: the pseudo-second-order kinetics model and the pseudo-
210 first-order kinetics model. In almost all MIPs for PFAS, the pseudo-second-order kinetics model fits the
211 experimental data better than the pseudo-first-order model. This indicates that the PFAS adsorption by the
212 MIPs follows chemical reaction mechanisms, such as electrostatic interactions reported between the selected
213 PFAS and MIP [30,38], in addition to hydrogen bonding and hydrophobic interactions in some cases
214 [27,36]. The results of adsorption kinetics studies of MIPs adsorbents for PFAS show that the time to reach
215 adsorption equilibrium ranges between 25 min [25] to 80 h [34]. This recorded time seems reasonable
216 compared to other types of adsorbents where similar or more prolonged time was required in some reports.
217 For example, GAC adsorbents required between 3 and 240 h to reach equilibrium [43,44], PAC adsorbents
218 reported equilibrium time between 1h and 24 h [45,46], resins adsorbents reached equilibrium after 2 to 168
219 h [44,47] and mineral adsorbents like clays reached equilibrium only after 0.3 h [48]. After the sorption
220 experiments, several synthesized MIPs were regenerated completely and re-used at least in five consecutive
221 adsorption-regeneration cycles without losing adsorption capacity for PFAS [35]. The MIP adsorbents
222 showed excellent mechanical stability and their practical applicability in direct removal from real water
223 samples was demonstrated.

224 ***2.3. Performances of the adsorbents***

225 The establishment of adsorption isotherms commonly allows the determination of the binding capacity of
226 sorbents. Several factors influence the binding capacity such as the physicochemical characteristics of the
227 sorbent (specific surface area, pore distribution, particle size), the solution temperature and pH and the
228 PFASs concentration. The binding capacity of MIPs for PFASs varies significantly, ranging from 1.289
229 [37] to 1455.5 mg·g⁻¹ [30] for PFOS and from 5.45 to 12.4 mg·g⁻¹ for PFOA as detailed in Table 2.

230 An important aspect of an adsorbent performance is its selectivity toward the target in a real media because
231 of the complexity of the matrix and the usually low concentration of the target in such medium. Improving
232 the selectivity will increase the performances of the adsorbent. The advantages of MIPs over other
233 adsorbents are expected to be their high affinity as well as their high specificity toward the target molecule
234 so they can isolate the target analyte from interfering species in a sample. The specific recognition process of
235 the MIPs adsorbent towards the template mainly depends on the adsorbent characteristics, e.g. the imprinted
236 cavities possessing distinct size and shape matching the targets and the specific functional groups involving
237 diverse interactions between the target and the MIP. Unlike traditional adsorbents and NIPs, MIPs benefit

238 from the presence of specific imprinted sites which can selectively extract targets from complex real
239 samples.

240 In a first step, the imprinting effect which is an indicator of the presence of specific binding cavities in the
241 MIP can be evaluated by comparing the binding capacity of the MIP with that of the corresponding NIP and
242 estimating the imprinting factor as the ratio of these two values. By doing so, as presented in table 2, it
243 appears that the PFAS binding capacity of MIPs goes from 1.01 [29] up to 4.95 [32]-fold higher than that of
244 the corresponding NIP in presence of the pure target. For instance, as shown in the Figure 4.a, maximum
245 PFOS binding capacity of MIP-CMSs ($75.99 \text{ mg}\cdot\text{g}^{-1}$) was almost two times that of NIP-CMSs ($43.94 \text{ mg}\cdot\text{g}^{-1}$),
246 indicating the specific binding property of the MIP-CMSs [38]. The studies of Cao and co-workers
247 enable a comparison between conventional AAM-based MIPs adsorbents prepared by precipitation
248 polymerization [28] and surface-imprinted MWCNTs-MIPs adsorbents [35] both prepared under
249 comparable conditions. MWCNTs-MIPs had an adsorption capacity toward PFOA 2.3-fold greater than the
250 conventional MIP. Moreover, the time to reach adsorption equilibrium for these MWCNTs-MIPs appears
251 to be 8-fold lower than in the case of the corresponding conventional AAM-based MIPs. In addition, the
252 maximum adsorption capacity of MWCNTs-MIPs ($12.4 \text{ mg}\cdot\text{g}^{-1}$) was almost two times that of MWCNTs-
253 NIPs ($7.44 \text{ mg}\cdot\text{g}^{-1}$), whereas, AAM-MIPs and AAM-NIPs have similar binding capacities with a imprinting
254 factor of only 1.08. This comparison clearly highlights the advantages of the surface imprinting technique.
255 In the surface imprinting method, the binding sites are accessible at the particles surface, which makes
256 rebinding and removal of target molecule in the polymer network quicker and easier.

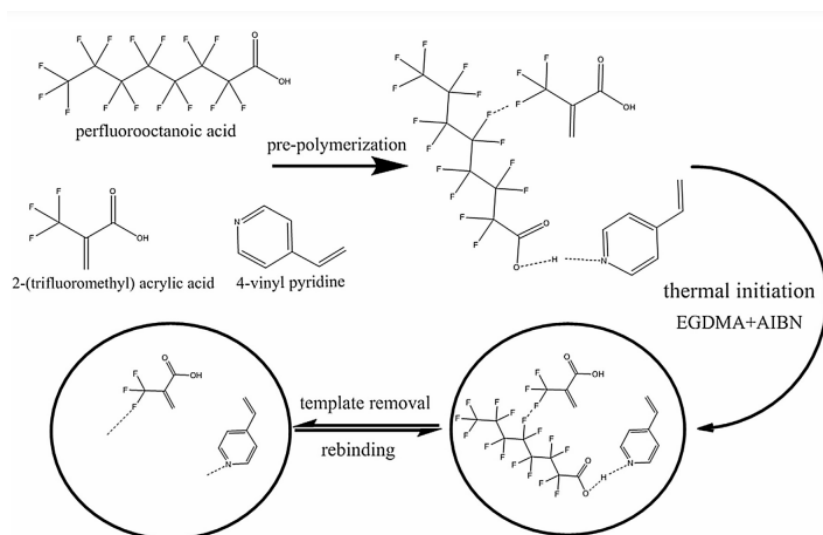
257 Comparing the adsorption capacities toward PFASs of MIP adsorbents with those of clay minerals shows
258 that the performances of MIPs are higher: clay minerals showed adsorption capacities ranging from 0.29 to
259 $0.31 \text{ mg}\cdot\text{g}^{-1}$ for PFOS and 0.10 to $0.11 \text{ mg}\cdot\text{g}^{-1}$ for PFOA [48]. However, MIPs binding capacities are lower
260 than those of other traditional adsorbents such as activated carbon or classical polymeric resins. For instance,
261 the reported adsorption capacity of GAC ranges from 71.6 to $290 \text{ mg}\cdot\text{g}^{-1}$ for PFOS and $41.3 - 120 \text{ mg}\cdot\text{g}^{-1}$
262 for PFOA while the PAC has an adsorption capacity around $560 \text{ mg}\cdot\text{g}^{-1}$ for PFOS and $290-500 \text{ mg}\cdot\text{g}^{-1}$ for
263 PFOA, whereas, resins showed adsorption capacities ranging between 200 to $2390 \text{ mg}\cdot\text{g}^{-1}$ for PFOS and
264 $525-1500 \text{ mg}\cdot\text{g}^{-1}$ for PFOA [26]. All these traditional sorbents usually suffer from a lack of selectivity
265 towards the targets; then other matrix components are co-extracted with target analytes. Only a limited
266 number of papers demonstrated the selectivity of traditional adsorbents to the class of PFAS compounds
267 [49–51]. The major limitation of these adsorbents is their lack of their selective ability toward one single
268 target PFAS from other PFAS molecules. From this perspective, MIPs appear to be a good choice to
269 improve the selectivity of the extraction process to one PFAS analyte from interferents.

270 The specificity of the MIPs is evaluated in presence of interferents in binary or multi-component
271 competitive solutions. Comparison of the removal rates of MIPs and NIPs for the template with respect to
272 the interferents shows that MIPs have higher specific binding preference toward the template against
273 interferents compared to NIPs. For several synthesized MIPs adsorbents for PFAS, it was found that other
274 contaminants with different molecular size, structures, functional groups and polarities such as phenol, 2,4-
275 dichlorophenoxy acetic acid [34,35], bisphenol A and dibutyl phthalate [40], sodium dodecylsulfate and
276 sodium dodecylbenzene-sulfonate [38] had little influence on the adsorption of the target. Moreover, when

277 other PFAS competitive pollutants having similar molecular structures were tested, the MIP adsorbents
278 showed significantly better selectivity toward the template compared to other PFAS interferents in single
279 and mixture solutions. However, the competitive PFAS with longer chains could also be adsorbed onto the
280 MIPs adsorbents in competition with shorter chain analogues [28,29,35]. For example, it was observed that
281 MIPs prepared for PFOA (8 carbons) showed higher adsorption rate towards long-chain PFASs such as
282 PFOS (8 carbons), PFNA (9 carbons), PFDA (10 carbons), PFUnA (11 carbons), PFDoA (12 carbons) than
283 short-chains PFASs like PFBS and PFBA (4 carbons), PFPeA (5 carbons), PFHxS and PFHxA (6 carbons),
284 PFHpA (7 carbons) (Figure 4.b). This might be due to the strong hydrophobicity of long-chain PFASs.

285 The practical applicability of MIP adsorbents in enrichment and separation was demonstrated by
286 performing direct removal of PFAS from real samples such as tap, lake and river water samples,
287 as well as human serum, pork or milk samples. The impurities in real environment can often
288 interfere with the binding of the analyte and decreases the adsorption efficiency. In real water
289 samples spiked with 5 μM PFOS, the removal rate of MMIPs and MSNs/MIPs toward PFOS
290 were in the range of 53.06-55.66% [36] and 61.68-76.12% [34] respectively. Excellent recovery
291 rates (77.0-96.4%) were obtained within human serum and water samples spiked in the
292 concentration range between 5 and 200 $\text{ng}\cdot\text{L}^{-1}$ [37]. In another example, the MWCNTs-MIPs
293 showed better recognition ability toward PFOA (removal rate of 74.3%) compared to
294 corresponding NIPs (removal rate of 38.1%) in tap water spiked with 100 $\mu\text{g}\cdot\text{L}^{-1}$ PFOA in a
295 mixture with other competitive PFAS[35]. For the detection of trace levels of long-chain PFAS
296 in pork sample and in milk, molecularly imprinted phenolic resins were used[31,32]. In pork sample,
297 PFOA was not detected in any of the prepared samples, PFNA was detected in six samples in the
298 concentration range of 5.21–19.04 $\text{ng}\cdot\text{g}^{-1}$, and PFDA was detected in three samples in the concentration
299 range of 0.13–0.72 $\text{ng}\cdot\text{g}^{-1}$. Whereas in milk sample, trace PFOA was detected in fifteen milk samples at
300 concentrations of 0.12–2.19 $\text{ng}\cdot\text{mL}^{-1}$, and PFOS was detected in four milk samples at concentrations of
301 0.08–0.31 $\text{ng}\cdot\text{mL}^{-1}$. These results confirm that molecularly imprinted polymers are selective and
302 accurate for determining trace levels of PFASs in complicated real samples.

303



304

305 **Fig. 2.** Synthesis scheme of a binary functional monomer MIP based on TFMMA and 4-VPy (Reprinted with
 306 permission from Elsevier, Copyright 2017 [29]).

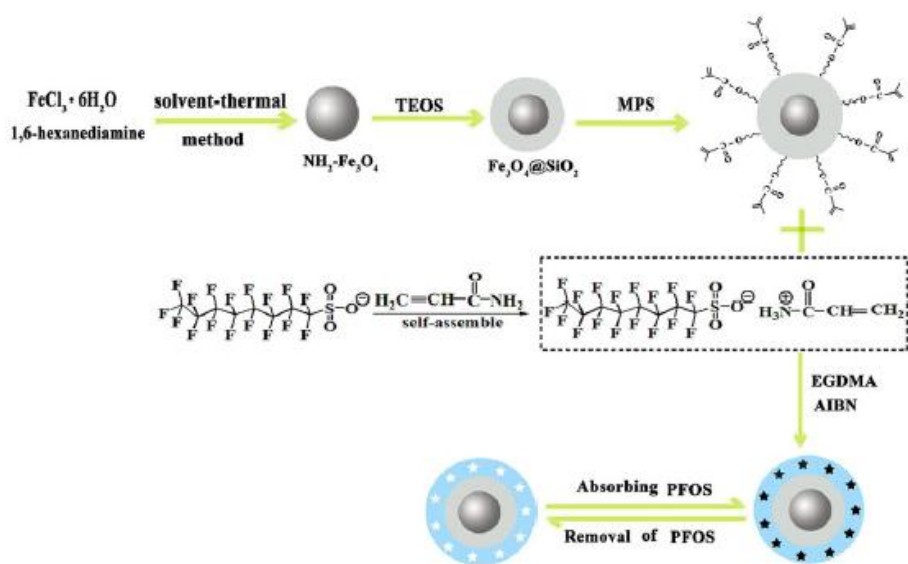


Fig. 3. Preparation process of MMIPs for PFOS (Reprinted with permission from John Wiley and
 Sons, Copyright 2017 [36]).

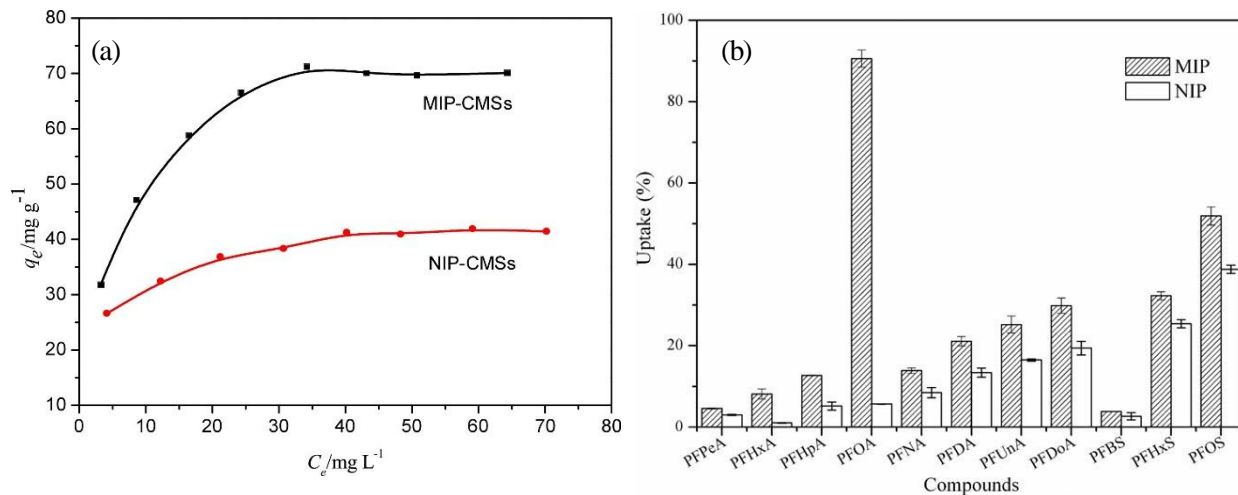


Fig. 4. (a) Adsorption isotherm of PFOS on MIP-CMSs and NIP-CMSs (Reprinted with permission from Science Direct, Copyright 2018 [38]). (b) Comparison of the adsorption capacity of PFOA with other PFASs on the MIP and NIPs adsorbents (Reprinted with permission from John Wiley and Sons, Copyright 2016[35]).

Table 2. Summary of PFAS absorption methods using MIPs, ^a Maximum adsorption capacity of MIP, ^b Maximum adsorption capacity of NIP, ^c Calculated imprinting factor (IF) = $\frac{Q_{e-MIP}}{Q_{e-NIP}}$

Template	Monomer	Crosslinker	Polymerization method	Q_{e-MIP}^a (mg.g ⁻¹)	Q_{e-NIP}^b (mg.g ⁻¹)	Imprinting factor ^c	Interferents	Reusability	Real samples	Mode of use	Ref
PFOA	-	ECH	Cross-linking of chitosan	1455.52	1203.51	1.21	PFOA, SDBS, phenol, 2,4-D, PCP,	5 cycles	-	Dispersive mode	[30]
PFOA or PFOS	4-VPy	EGDMA or TRIA	Bulk polymerization	-	-	-	2,4-D	-	-	Dispersive mode	[27]
PFOA	AAM	EGDMA	Precipitation polymerization	5.45	5.04	1.08	PFPeA, PFHxA, PFHpA, PFNA, PFDA, PFUnA, PFDoA, PFBS, PFHxS, PFOS	5 cycles	-	Dispersive mode	[28]
PFOA	4-Vpy and TFMAA	EGDMA	Precipitation polymerization	6.42 for PFOA 6.27 for PFOS	6.31 for PFOA 5.31 for PFOS	1.01 1.18	PFPA, PFHxA, PFOA, PFNA, PFDA, PFUnA, PFDoA, PFOS, PFBS, PFHxS	5 cycles	Spiked lake water (1 mg.L ⁻¹)	Dispersive mode	[29]
PFOS	AAM	EGDMA	Surface imprinting	2.401	1.164	2.06	PFOA, SDBS	SDS, 5 cycles	Spiked tap and river water (5 μM)	Dispersive mode	[36]
PFOS	Dopamine	-	Self-polymerization of dopamine	1.289 for Low affinity binding site 0.556 for high affinity binding site	0.331	1.75	PFOA, SDBS, CTAB, phenol, PFHxS, F-53B	5 cycles	Spiked lake water, river water, human serum (5-200 ng/L)	SPE	[37]

PFOS	APTES	TEOS	Surface imprinting	21.10	9.78	2.15	PFOA, SDS, 5 cycles SDBS	Spiked tap and river water (5 mode μM)	Dispersive	[34]
PFOS	MTAC TFMAA	and MBA	Surface imprinting	75.99	43.94	1.72	PFOA, PFHSB, 4 cycles PFKSB, F53-B, BPA, DBP, NP	-	Dispersive mode	[38]
PFOA	AAM	EGDMA	Surface imprinting	12.4	7.44	1.69	PFPeA, 5 cycles PFHxA, PFHpA, PFNA, PFDA, PFBS, PFHxS, PFOS	Spiked tap water ($100 \mu\text{g.L}^{-1}$)	Dispersive mode	[35]
PFOA	AAM	EGDMA	Surface imprinting	0.8125 ($\mu\text{g.cm}^{-1}$)		-	PFOS, PFHA, 2,4-D		Dispersive mode	[40]
PFOA	MAA	TRIM	Surface imprinting		-	-	PFBA, PFeA, PFOA, PFHxA, PFHpA		Dispersive mode	[39]
PFTeDA	4- mercaptophenol	Glutaraldehyde	Bulk polymerization				Atraton, Prometryn, Sulfamethoxazole, β -Estradiol	Pork samples	Dispersive SPE	[31]
PFNA	<i>m</i> -aminophenol	Glutaraldehyde	Bulk polymerization	-	-	4.95 for PFOA 3.76 for PFOS	Sulfamethazine, sulfamethoxazole, florfenicol, thiamphenicol	Milk samples	Dispersive filter extraction	[32]

313 **3. MIPs as selective sensing materials for PFAS**

314 In recent years, new sensor technologies have emerged to try to address the challenge of PFAS detection as
315 a more deployable means to monitoring these pollutants. Innovations include colorimetric sensing [52], pre-
316 cursor detection using the total oxidisable precursor assay [53] and MIP-based sensors. The following
317 section summarizes MIP-based sensor materials created for PFAS detection in aqueous environments
318 according to their detection type.

319 **3.1. Electrochemical sensors**

320 Electrochemical transduction plays a big role in diversifying sensors technology for bioanalytical and
321 environmental applications [54,55]. The immobilization of MIPs on the surface of electrodes offers an
322 alternative to biomolecule-based materials, potentially overcoming classical sensing challenges related to
323 biological recognition such as high cost, instability and selectivity [56–59].

324 To date, only a few publications have been reported for PFAS-specific detection (Table 3). It is interesting
325 to note that all the strategies reported for PFAS sensing rely on soft (non-crosslinked), electroactive
326 polymers, that are often produced using electropolymerisation methods. This approach offers several
327 advantages compared to chemical polymerization methods, namely the use of aqueous solvents, control of
328 the polymer layer characteristics such as thickness, conductivity etc. and good adhesion to the base electrode
329 material [60]. Electrochemical synthesis of MIPs using *o*-phenylenediamine (oPD) (also known as 1,2-
330 benzenediamine) as a starting material has been reported as a promising approach to MIP synthesis. Indeed
331 the homopolymer of *o*-phenylenediamine (poly(*o*-phenylenediamine)) was one of the first examples of
332 electrochemically synthesized MIPs, and was used for the selective detection of glucose [61]. Their polymer
333 films are considered rigid and stable. Poly-oPD (Figure 4) is non-conductive at pH 5.2, making it a good
334 candidate for capacitance-based sensors [62]. oPD is typically electropolymerized via cyclic voltammetry
335 from aqueous solutions on gold or carbon electrodes [63–66] in the presence of PFAS. PFAS is then
336 removed from these films by a wash step (typically water/methanol), and binding of target is monitored
337 indirectly via a bulk redox probe response such as ferrocenecarboxylic acid. Limit of detection (LOD)
338 values as low as $7.5 \times 10^{-3} \mu\text{g.L}^{-1}$ (0.015 nM) for PFOS have been reported using this strategy, falling well
339 below the limit of $0.4 \mu\text{g.L}^{-1}$ set by the WHO [10] for drinking water. It is also noteworthy that this kind of
340 MIP-based sensors can be enhanced by surface modification of the electrode surface with nanomaterials,
341 such as gold nanostars (AuNS) [64]. Selectivity studies [63–65] considered structurally similar interfering
342 analytes to PFOS (some belonging to the PFAS class and others not) and revealed that PFOS-MIP sensors
343 exhibited high affinity towards PFOS compared to non-PFAS interferents, and a lesser selectivity towards
344 PFOS when smaller PFAS interferents were present simultaneously, due to a more favourable competing
345 access to binding sites. Thus, this sensing approach is promising for detecting PFAS in contaminated water,
346 but further enhancement of selectivity remains a challenge to discriminate between the different PFAS,
347 when present in water as a mixture.

348 The conducting polymer polyaniline (PANI) (Figure 4) has also been used as a soft MIP templating
349 material for several targets [67–70,59]. A paper-based MIP sensor was reported recently for PFOS
350 detection, created through the chemical polymerization of PANI in the presence of PFOS [71]. Aniline

351 (An)/PFOS was first adsorbed onto the polyester paper substrate, then exposed to oxidant and dopant to
352 create the PFOS encapsulated polymer film. Upon removal of PFOS, the MIP was created whereby, in the
353 presence of PFOS, which is a negative-charge-rich aliphatic acid, PANI conductivity was modulated
354 through PFOS binding. It was proposed that PFOS binding occurred through the electron holes on the
355 nitrogen atoms of aniline, reducing the number of charge carriers on the surface in the film, reducing film
356 conductivity. This sensor had a reported LOD of 1.02 nM, and resistivity tests before and after exposure to
357 spiked water samples showed significant selectivity towards PFOS compared to other PFAS .

Table 3. Summary of MIP-based PFAS sensing approaches, highlighting the sensor type, monomer and crosslinking materials, polymerization method, substrate, target PFAS, detection method, limit of detection (LoD), linear dynamic range, spiked water samples tested and recovery

Sensor type	Monomer	Crosslinker	Polymerization method	Substrate	Target molecule	Detection method	LoD ($\mu\text{g.L}^{-1}$)	Linear dynamic range ($\mu\text{g.L}^{-1}$)	Spiked water sample	Recovery rate	Ref
Electrochemical	oPD	–	Electropolymerization	GCE	PFOS	Voltammetry	0.025	0–0.025	–	–	[63]
	oPD	–	Electropolymerization	GCE	PFOS	Voltammetry	7.5×10^{-3}	0.025–2.5	Deionised, tap	86–93 %	[64]
	oPD	–	Electropolymerization	Au disc electrode	PFOS	Voltammetry	0.02	0.05–2.45 and 4.75–750	Distilled, tap, bottled	82–110 %	[65]
	oPD	–	Electropolymerization	Au-SPE	PFOS	Voltammetry	–	–	–	–	[66]
	An	–	Radical polymerization	Polyester substrate	PFOS	Resistivity	1.02×10^{-3}	10^{-3} – 10^{-2}	–	–	[71]
	Py	–	Electropolymerization	Graphite electrode	PFOA	Potentiometry	41.407	4.14×10^3 –4.14	–	–	[72]

Photoelectrochemical	Aam	EGDMA	Photopolymerization	FTO glass	PFOA	Photocurrent response	0.01	0.02 – 1000	Tap, river	98 – 102 %	[73]
	Aam	EGDMA	Photopolymerization	C-SPE	PFOSF	Photocurrent response	0.01	0.05 – 500	Tap, river, lake	92 – 100 %	[74]
	Aam	EGDMA	Photopolymerization	TiO ₂ NTAs	PFOS	Photocurrent response	86	250 – 5000	Tap, river, mountain	95 – 117 %	[75]
Electrochemiluminescent	Py	–	Electropolymerization	GCE	PFOA	Electrochemiluminescence	0.01	0.02 – 40 and 50 – 400	Tap, river, lake	96.9 – 103.8%	[76]
Photoluminescent	APTS	–	Anchoring APTS-FITC conjugates with/without PFOS at surface of SiO ₂ NPs	SiO ₂ NPs	PFOS	Fluorescence	5.57	5.57 – 48.54	Tap, river	95.7 – 101 %	[77]
	Chitosan	ECH	Hydrothermal sol-gel polymerization	Chitosan hydrogel	PFOS	Fluorescence	4×10^{-7}	$2 \times 10^{-5} - 2 \times 10^{-4}$	Serum, urine	81 – 98 %	[78]
	APTES	TEOS	Sol-gel polymerization	Silica shell	PFOA	Photoluminescence	10.35	$1.03 \times 10^2 - 6.2 \times 10^3$	–	91 – 107 %	[79]
Surface plasmon resonance	VBT and PFDA	EGDMA	Thermal polymerization	POF	PFOA	Surface plasmon resonance	0.13	–	–	–	[80]

360 Polypyrrole (Ppy) (Figure 4) is another widely used conducting polymer in sensing applications [62]. A
361 potentiometric sensor based on Ppy electrodeposited on pencil lead in the presence of PFOA as template
362 was developed to detect fluoro-surfactants from aqueous firefighting foams [72]. Methylene blue was
363 incorporated into the Ppy matrix during electropolymerisation to increase selectivity (forming ion pairs with
364 the anionic surfactants of interest that were only sparingly soluble in water). The PFOA-specific MIPs
365 showed good selectivity towards PFOA compared to 6:2 fluorotelomer sulfonate (6:2 FTS) and PFOS
366 (which has a larger hydrophilic moiety of the sulfonic acid than the carboxylic acid in PFOA). It also
367 showed an interesting response towards SDS and sodium dodecylbenzenesulfonate (SDBS) (both common
368 detergents), which falls outside the scope of this review. However, the SDS-MIP showed no discernible
369 response for smaller interferent molecules, i.e. PFOA, PFOS, 6:2FTS and SDBS, because SDS leaves a
370 larger cavity after its removal, allowing the smaller interferents to bind to the MIP cavities. Thus, the sensor
371 showed great potential as an accessible pre-screening tool for detecting anionic surfactants. However, efforts
372 to test it in water samples instead of aqueous or buffered solutions remain crucial to validate its efficiency.

373 **3.2. Photoelectrochemical sensors**

374 Photoelectrochemical (PEC) sensors have evolved from electrochemistry and exploit the effect of light on
375 photoactive materials to drive photo-induced chemical events associated with charge separation and transfer
376 [81,82]. PFAS has been the target for several MIP-based PEC sensing approaches [73,83,74,75]. The MIP
377 material is based on photopolymerized AAM crosslinked with EGDMA using azobisisobutyronitrile as
378 initiator. In one publication reporting a PEC sensor targeting PFOS, the photoactive material consisted of a
379 highly ordered, vertically aligned TiO₂ NTA serving as a graft polymerization substrate for the Aam-based
380 MIPs [75]. Evaluating the relative change in photocurrent response to PFOS against that of PFAS analogues
381 and non-fluorinated interferents indicated high binding selectivity for PFOS, even when interferent
382 concentration was 20 times greater than PFOS. Sensor repeatability was 2.8 % standard deviation for 10
383 measurements, and long-term stability after 1 month storage (< 4 % decrease in response) and 3 months
384 storage (<5.1 %). The LOD of this sensor was estimated at 86 µg.L⁻¹.

385 In another PEC-based PFAS sensor, an AgI nanoparticle and BiOI nanoflake array (AgI-BiOINFs)
386 immobilised on fluorine-doped tin oxide (FTO) was used as a photoactive electrode and was realised via a
387 successive ionic layer adsorption and reaction method [73]. The array was subsequently grafted with a
388 PFOA MIP. The LOD for PFOA was estimated at 0.01 µg.L⁻¹, comparable to that achievable with LC-
389 MS/MS. Selectivity towards PFOA was remarkable as the relative change in the photocurrent response of
390 samples containing selected structurally similar non-fluorinated compounds and other PFOA analogues was
391 negligible compared to PFOA-spiked samples. Furthermore, in the presence of interferent compounds, the
392 response to PFOA was not impacted and the superior selectivity for PFOA was attributed to the selective
393 shape and hydrogen bond identification. The recovery rate for spiked tap and river water samples was
394 reported to be in the range of 98.2-102.4 %. The same group later proposed a disposable PEC sensor for
395 PFOSF using a screen-printed carbon electrode functionalised with electrodeposited BiOINF [74] (Figure
396 5). This surface was then used for grafting the MIP. This method was simpler to realize and offered high
397 selectivity to PFOSF with a 0.01 µg.L⁻¹ LOD, much lower than the 0.5 µg.L⁻¹ reported by LC-MS.

398 **3.3. Electrochemiluminescent sensors**

399 The basic principle of electrochemiluminescence (ECL) is that an electrochemically initiated reaction
400 produces molecules at excited states that undergo subsequent relaxation and generate a luminescence
401 emission [84,85]. The smart combination of electrochemistry and chemiluminescence gives ECL several
402 advantages, mainly in avoiding background noise and issues associated with light scattering as it does not
403 require an external light source [85]. Much like PEC sensors, ECL detection using MIPs as selective
404 materials has received considerable attention as an analytical tool for clinical detection of analytes like
405 deoxyribonucleic acid [86], cancer biomarkers [87], bacteria [88] and antibodies [89]. However, reports
406 on MIP-based ECL sensors for PFAS targets in environmental waters are still scarce [90]. One recent
407 example was based on MIP-modified ultrathin graphitic carbon nitride nanosheets (utg-C₃N₄) for the
408 detection of PFOA [76]. The method consisted of modifying a glassy carbon electrode (GCE) with a utg-
409 C₃N₄ dispersion using drop-casting and subsequently carrying out an electropolymerisation of 5 mM pyrrole
410 and 1 mM PFOA via cyclic voltammetry at pH 6. The ECL signal intensity was shown to decrease with
411 increased concentrations of PFOA in a linear fashion over two concentration ranges: 0.02 to 40 ng.ml⁻¹ and
412 50-400 ng.ml⁻¹. The LOD was estimated to be 0.01 ng.ml⁻¹, significantly lower than those reported using
413 chromatographic methods (25 ng.L⁻¹ by LC-MS/MS, for example [91]). The selectivity of the ECL sensor
414 was evaluated, and it was found that the change in ECL intensity was negligible for interfering compounds
415 with similar size and structure to PFOA. Recovery rates in samples of spiked tap, river and lake water were
416 found between 96.9 and 103.8%. The reproducibility and stability of the sensors were investigated, and the
417 RSD was found to be 4.10%.

418

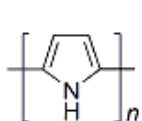
419 **3.4. Photoluminescent sensors**

420 Fluorescence-based detection methods have received considerable attention thanks to their remarkable
421 sensitivity and versatility in terms of transduction schemes [92,93]. Fluorescent sensors have utilized
422 quantum dots (QDs) [94], nanomaterials [95], conjugated polymers [93] and photoluminescent MIPs
423 (PLMIPs) [96]. There are numerous ways to synthesize PLMIPs, most of which involve copolymerization
424 of fluorescent monomers, or encapsulation with fluorophores or nanomaterials [96]. For instance, a
425 selective detection method for PFOS in water through MIP-capped silica nanoparticles was published [77].
426 Fluorescein 6-isothiocyanate (FITC) dye was covalently linked to the surface of silica nanoparticles (SiO₂-
427 NPs). Upon binding of PFOS to NH₂ ligands within the specific recognition site, the PFOS-amine
428 complexes formed strongly suppressed the fluorescence emission of the FITC through a charge-transfer
429 mechanism from FITC to PFOS. The LOD was determined to be 5.57 µg.L⁻¹. Analysis of tap and river
430 water spiked with PFOS revealed a recovery rate from 95.7 to 101%. For samples containing a mixture of
431 PFOS and interfering molecules (PFOA, PFHxA, PFHxS, Phenol, SDBS), the quantitative recovery of
432 PFOS ranged from 97.9 to 106%. Another similar approach for detecting PFOS was developed using a
433 MIP-based fluorescent hydrogel comprising carbon quantum dot (CQD)-doped chitosan [78]. However, it
434 seemed that both the MIP- and NIP-coated CQDs showed fluorescence responses to PFOS, which indicated
435 that the NH₂ groups present at the surface of the MIP- and NIP-coated NPs could also act as binding sites
436 for PFOS through hydrogen bonding and electrostatic interactions. Despite this, as shown through the

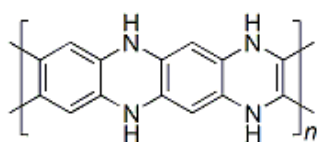
437 imprinting factor (IF) ($K_{SV, MIP}/K_{SV, NIP}$), the specific binding cavities in the MIP hydrogel had stronger
438 adsorption of PFOS and showed higher fluorescence intensities where IF value for analogue molecules
439 ranged from 0.51 to 1.33, compared to 2.75 for PFOS. Cadmium-telluride (CdTe)/cadmium-sulphide
440 (CdS)-based QDs coated with thioglycolic acid (TGA), imprinted with 3-aminopropyltriethoxysilane
441 (APTES) in the presence of PFOA have been reported via sol-gel polymerization [79]. The PL intensity of
442 the MIP-capped QDs decreased by 44% with PFOA bound to the recognition sites compared to the NIP-
443 capped QDs. However, this PL intensity soars to 81.25% after the removal of PFOA, thus confirming the
444 capacity to which PFOA can quench the MIP-capped CdTe/CdS QDs. The PFOA-induced PL quenching
445 was significantly higher than those resulting from analogues using the MIP-capped QDs, however the
446 response was nearly identical using the NIP-capped QDs for these same analogues. Analysis of real water
447 samples showed average recovery rates of PFOA ranging between 91-107% with RSD below 5.6%.

448 Overall, these PL sensors showed value in coupling selective recognition of MIPs and analyte-dependent
449 emission of various fluorophores such as QDs and fluorescent dyes, which allows for more applications in
450 the optical detection of PFAS in real water samples.

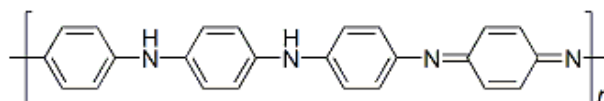
451



polypyrrole (PPy)



poly-ortho-phenylenediamine (Poly-*o*PD)
(benzenoid unit)



polyaniline (PANI)
(emeraldine base)

452

Fig. 4 Chemical structures of (a) Ppy, (b) Poly-oPD, and (c) PANI

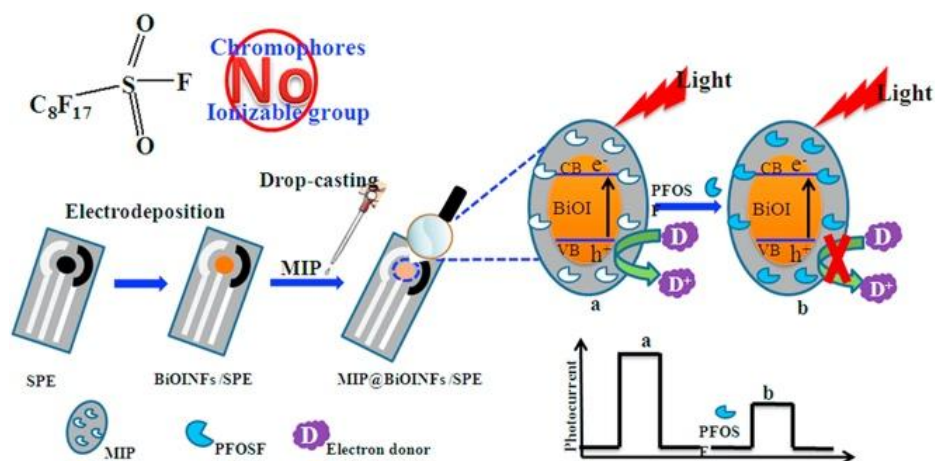


Fig. 5. Schematic of photoelectrochemical detection of PFOSF using a MIP based BiOINFs on SPE sensing strip (Reprinted with permission from Elsevier, Copyright 2018 [74]).

342 **3.5. Surface plasmon resonance (and optical intensity-based sensors)**

343 One of the relatively new optical detection methods is plasmon surface resonance (SPR). Popularized in the
344 90s by biosensor companies [97], this refractive index-based technique allows the determination of the
345 kinetic parameters of molecular interactions. However, it can also be used for real-time, label-free analysis
346 of analytes in complex matrices with superior sensitivity [97,98]. The integration of MIPs to SPR sensors
347 was very favorable and shifted research to achieve more sensitive detection. However, most of this research
348 is geared toward detecting complex biomolecules and biomolecular assays, such as proteins [98,99],
349 antigens [100], and antibiotics [101]. There are very few studies done to detect pollutants and non-biological
350 analytes using SPR and MIPs, namely explosives [102], pesticides [103,104], and PFAS. The latter received
351 attention with the recent development of a MIP based plasmonic plastic optical fiber (POF) sensor to detect
352 PFOA in water [80]. In this method, the optical platform consists of a POF (poly(methyl methacrylate))
353 topped with an optical (photoresist) buffer layer (1.5 μm) and finished off with a sputtered thin gold film (60
354 nm in thickness). The photoresist optical layer enhances the sensor's performance by offering a higher
355 refractive index than the POF core in the desired visible range. On the other hand, the gold film provides a
356 support to the MIP receptor layer, whereby it can be directly deposited (in-situ polymerization) without any
357 prior surface modification, which is a key advantage for this kind of sensors. Thus, the binding of the target
358 analyte to the recognition site in the MIP layer causes a change in the refractive index between this layer and
359 the gold film, which causes a shift in the resonance wavelength (which can be quantified through SPR
360 spectroscopy). However, when PFOA was present in the bulk solution, the change in resonance wavelength
361 (and refractive index) recorded was a decrease rather than the usual increase. The success of this sensor was
362 confirmed by binding and non-binding experiments, where the signal recorded with the SPR-POF-NIP
363 showed no shift of the resonance wavelength, whereas the SPR-POF-MIP showed a clear shift into smaller
364 values (decrease in refractive index), with an LoD of $0.13 \mu\text{g.L}^{-1}$, comparable with that of an SPR-POF
365 platform with a bio-receptor (antibody) of $0.24 \mu\text{g.L}^{-1}$, previously developed by the same research team for
366 the detection of PFOA [105].

367 This SPR-POF-MIP sensor also showed similar responses when adding PFAS compounds with varying
368 carbon chain lengths (C4-C11), compared to PFOA alone in the sample solutions, with a slight difference in
369 resonance wavelength variation that can be explained with the change in refractive index in the MIP layer
370 due to the change in molecular size of the binding analyte present.

371 In a similar study done by the same group [106], an intensity-based POF sensor paired with a MIP receptor
372 was used for the first time to detect C4 to C12 PFAS in water samples. This POF-MIP sensor is virtually
373 identical to the SPR-POF-MIP discussed previously [80], except for the gold film and optical buffer layer
374 (which provide the SPR properties) and the spin-coated MIP layer on the POF platform. This type of
375 detection showed promise for PFAS detection in water samples, offering a lower cost of preparation and
376 experimental set-up, convenience to use under environmental conditions and good repeatability.

377 **4. Conclusions**

378 PFAS are emerging as chemicals of concern because of the reported risks to human health, notably their
379 capacity to act as endocrine disruptors, and their environmental safety as they are persistent and

380 bioaccumulative. PFOA and PFOS are of particular interest as they are very widely used in the
381 manufacture of household objects, cleaning supplies and as firefighting foams.

382 MIPs are popular as selective recognition elements due to their unique ability to bind specific targets with
383 high affinity. As traditional adsorption materials for PFAS, such as activated carbon, biomaterials and
384 mineral materials, lack in selectivity, MIPs were introduced as an alternative for more efficient enrichment
385 methods of PFAS. The methods of MIP preparation range from traditional polymerization techniques such
386 as bulk and precipitation polymerization, to more innovative ones like surface imprinting techniques
387 involving functionalized nanomaterials (such as MWCNTs and CMSs). Many of the PFAS-MIP sensors
388 reviewed here exhibit higher affinity towards PFAS than for competing minerals present in sample matrix -
389 river, lake, sea water. Lab testing is performed on collected water samples typically and on-site testing is less
390 common. However, when the field moves onto this, no doubt more challenges will arise. High selectivity
391 towards PFAS is particularly evident when in competition with structurally related non-PFAS. As for
392 competing PFAS pollutants, long-chained molecules are more likely to bind to PFAS-MIPs than to their
393 short-chained analogues. Moreover, regeneration studies on some PFAS-MIPs do demonstrate reusability
394 with conserved adsorption capacity and mechanical stability, further highlighting the advantages of using
395 MIPs as selective sorbents. The reported detection methods used included electrochemical,
396 photoluminescent, photoelectrochemical, electrochemiluminescent, and surface plasmon-based strategies.
397 This versatility is a further advantage as it provides alternatives for industrial scale sensor manufacture.
398 Finally, it is important to stress that while MIP-based sensors will never replace traditional, more established
399 detection techniques, PFAS-MIP sensors inherently present advantages in terms of portability,
400 miniaturisation and cost-effectiveness. Although sensor technology is always more challenged in terms of
401 analytical sensitivity, there are some reports emerging of PFAS-MIP sensors with sensitivities reaching ppb
402 and even ppt levels, targets that must be delivered upon to comply with PFAS regulations.

403

404

405 **Acknowledgements**

406 This work was financially supported by NEMO ERANET MarTERA research program, funded by the
407 ANR (ANR-20-MART-0001) and the Marine Institute.

408

409 **References**

- 410 [1] N. Ding, S.D. Harlow, J.F. Randolph Jr, R. Loch-Carus, S.K. Park, Perfluoroalkyl and polyfluoroalkyl
411 substances (PFAS) and their effects on the ovary, *Hum. Reprod. Update.* 26 (2020) 724–752.
412 <https://doi.org/10.1093/humupd/dmaa018>.
- 413 [2] E. Gagliano, M. Sgroi, P.P. Falciglia, F.G.A. Vagliasindi, P. Roccaro, Removal of poly- and perfluoroalkyl
414 substances (PFAS) from water by adsorption: Role of PFAS chain length, effect of organic matter and
415 challenges in adsorbent regeneration, *Water Res.* 171 (2020) 115381-115411.
416 <https://doi.org/10.1016/j.watres.2019.115381>.
- 417 [3] R.C. Buck, J. Franklin, U. Berger, J.M. Conder, I.T. Cousins, P. de Voogt, A.A. Jensen, K. Kannan, S.A.
418 Mabury, S.P. van Leeuwen, Perfluoroalkyl and polyfluoroalkyl substances in the environment: Terminology,
419 classification, and origins, *Integr. Environ. Assess. Manag.* 7 (2011) 513–541.
420 <https://doi.org/10.1002/ieam.258>.
- 421 [4] P. Zareitalabad, J. Siemens, M. Hamer, W. Amelung, Perfluorooctanoic acid (PFOA) and
422 perfluorooctanesulfonic acid (PFOS) in surface waters, sediments, soils and wastewater – A review on

- 423 concentrations and distribution coefficients, *Chemosphere*. 91 (2013) 725–732.
424 <https://doi.org/10.1016/j.chemosphere.2013.02.024>.
- 425 [5] W. Völkel, O. Genzel-Boroviczeny, H. Demmelmair, C. Gebauer, B. Koletzko, D. Twardella, U. Raab, H.
426 Fromme, Perfluorooctane sulphonate (PFOS) and perfluorooctanoic acid (PFOA) in human breast milk:
427 Results of a pilot study, *Int. J. Hyg. Environ. Health*. 211 (2008) 440–446.
428 <https://doi.org/10.1016/j.ijheh.2007.07.024>.
- 429 [6] B.D. Key, R.D. Howell, C.S. Criddle, Defluorination of Organofluorine Sulfur Compounds by *Pseudomonas*
430 Sp. Strain D2, *Environ. Sci. Technol.* 32 (1998) 2283–2287. <https://doi.org/10.1021/es9800129>.
- 431 [7] H.Fr. Schröder, R.J.W. Meesters, Stability of fluorinated surfactants in advanced oxidation processes—A follow
432 up of degradation products using flow injection–mass spectrometry, liquid chromatography–mass
433 spectrometry and liquid chromatography–multiple stage mass spectrometry, *J. Chromatogr. A*. 1082 (2005)
434 110–119. <https://doi.org/10.1016/j.chroma.2005.02.070>.
- 435 [8] Directive 2013/39/EU of the European Parliament and of the Council of 12 August 2013 amending Directives
436 2000/60/EC and 2008/105/EC as regards priority substances in the field of water policy/Text with EEA
437 relevance, (n.d.) 17.
- 438 [9] Environmental Protection Agency (EPA), Provisional Health Advisories for Perfluorooctanoic acid (PFOA) and
439 Perfluorooctane Sulfonate (PFOS), (n.d.). [http://](http://water.epa.gov/action/advisories/drinking/upload/2009_01_15_criteria_drinking_pha_PFOA_PFOS.PDF)
440 water.epa.gov/action/advisories/drinking/upload/2009_01_15_criteria_drinking_pha_PFOA_PFOS.PDF.
- 441 [10] European Commission, Proposal for a DIRECTIVE OF THE EUROPEAN PARLIAMENT AND OF THE
442 COUNCIL on the quality of water intended for human consumption (recast), (2018).
- 443 [11] D.M. Lemal, Perspective on Fluorocarbon Chemistry, *J. Org. Chem.* 69 (2004) 1–11.
444 <https://doi.org/10.1021/jo0302556>.
- 445 [12] J.C. Biffinger, H.W. Kim, S.G. DiMaggio, The Polar Hydrophobicity of Fluorinated Compounds,
446 *ChemBioChem*. 5 (2004) 622–627. <https://doi.org/10.1002/cbic.200300910>.
- 447 [13] K.H. Kucharzyk, R. Darlington, M. Benotti, R. Deeb, E. Hawley, Novel treatment technologies for PFAS
448 compounds: A critical review, *J. Environ. Manage.* 204 (2017) 757–764.
449 <https://doi.org/10.1016/j.jenvman.2017.08.016>.
- 450 [14] A.F. Ojo, C. Peng, J.C. Ng, Assessing the human health risks of per- and polyfluoroalkyl substances: A need for
451 greater focus on their interactions as mixtures, *J. Hazard. Mater.* 407 (2021) 124863–124876.
452 <https://doi.org/10.1016/j.jhazmat.2020.124863>.
- 453 [15] N.M. Crawford, S.E. Fenton, M. Strynar, E.P. Hines, D.A. Pritchard, A.Z. Steiner, Effects of perfluorinated
454 chemicals on thyroid function, markers of ovarian reserve, and natural fertility, *Reprod. Toxicol.* 69 (2017) 53–
455 59. <https://doi.org/10.1016/j.reprotox.2017.01.006>.
- 456 [16] K. Haupt, K. Mosbach, Molecularly Imprinted Polymers and Their Use in Biomimetic Sensors, *Chem. Rev.* 100
457 (2000) 2495–2504. <https://doi.org/10.1021/cr990099w>.
- 458 [17] K. Karim, F. Breton, R. Rouillon, E.V. Piletska, A. Guerreiro, I. Chianella, S.A. Piletsky, How to find effective
459 functional monomers for effective molecularly imprinted polymers?, *Adv. Drug Deliv. Rev.* 57 (2005) 1795–
460 1808. <https://doi.org/10.1016/j.addr.2005.07.013>.
- 461 [18] A. Poma, A.P.F. Turner, S.A. Piletsky, Advances in the manufacture of MIP nanoparticles, *Trends Biotechnol.*
462 28 (2010) 629–637. <https://doi.org/10.1016/j.tibtech.2010.08.006>.
- 463 [19] D. Refaat, M.G. Aggour, A.A. Farghali, R. Mahajan, J.G. Wiklander, I.A. Nicholls, S.A. Piletsky, Strategies for
464 Molecular Imprinting and the Evolution of MIP Nanoparticles as Plastic Antibodies—Synthesis and
465 Applications, *Int. J. Mol. Sci.* 20 (2019) 6304–6324. <https://doi.org/10.3390/ijms20246304>.
- 466 [20] A. Azizi, C.S. Bottaro, A critical review of molecularly imprinted polymers for the analysis of organic pollutants
467 in environmental water samples, *J. Chromatogr. A*. 1614 (2020) 460603–460637.
468 <https://doi.org/10.1016/j.chroma.2019.460603>.
- 469 [21] O.S. Ahmad, T.S. Bedwell, C. Esen, A. Garcia-Cruz, S.A. Piletsky, Molecularly Imprinted Polymers in
470 Electrochemical and Optical Sensors, *Trends Biotechnol.* 37 (2019) 294–309.
471 <https://doi.org/10.1016/j.tibtech.2018.08.009>.
- 472 [22] X. Shen, L. Zhu, N. Wang, L. Ye, H. Tang, Molecular imprinting for removing highly toxic organic pollutants,
473 *Chem Commun.* 48 (2012) 788–798. <https://doi.org/10.1039/C2CC14654A>.

- 474 [23] Y. Fuchs, O. Soppera, K. Haupt, Photopolymerization and photostructuring of molecularly imprinted polymers
475 for sensor applications—A review, *Anal. Chim. Acta.* 717 (2012) 7–20.
476 <https://doi.org/10.1016/j.aca.2011.12.026>.
- 477 [24] Q. Yu, R. Zhang, S. Deng, J. Huang, G. Yu, Sorption of perfluorooctane sulfonate and perfluorooctanoate on
478 activated carbons and resin: Kinetic and isotherm study, *Water Res.* 43 (2009) 1150–1158.
479 <https://doi.org/10.1016/j.watres.2008.12.001>.
- 480 [25] Z. Du, S. Deng, Y. Bei, Q. Huang, B. Wang, J. Huang, G. Yu, Adsorption behavior and mechanism of
481 perfluorinated compounds on various adsorbents—A review, *J. Hazard. Mater.* 274 (2014) 443–454.
482 <https://doi.org/10.1016/j.jhazmat.2014.04.038>.
- 483 [26] D.Q. Zhang, W.L. Zhang, Y.N. Liang, Adsorption of perfluoroalkyl and polyfluoroalkyl substances (PFASs)
484 from aqueous solution - A review, *Sci. Total Environ.* 694 (2019) 133606-133622.
485 <https://doi.org/10.1016/j.scitotenv.2019.133606>.
- 486 [27] S. Deng, D. Shuai, Q. Yu, J. Huang, G. Yu, Selective sorption of perfluorooctane sulfonate on molecularly
487 imprinted polymer adsorbents, *Front. Environ. Sci. Eng. China.* 3 (2009) 171–177.
488 <https://doi.org/10.1007/s11783-009-0017-4>.
- 489 [28] F. Cao, L. Wang, X. Ren, H. Sun, Synthesis of a perfluorooctanoic acid molecularly imprinted polymer for the
490 selective removal of perfluorooctanoic acid in an aqueous environment, *J. Appl. Polym. Sci.* 133 (2016)
491 43192-43201. <https://doi.org/10.1002/app.43192>.
- 492 [29] F. Cao, L. Wang, Y. Tian, F. Wu, C. Deng, Q. Guo, H. Sun, S. Lu, Synthesis and evaluation of molecularly
493 imprinted polymers with binary functional monomers for the selective removal of perfluorooctanesulfonic acid
494 and perfluorooctanoic acid, *J. Chromatogr. A.* 1516 (2017) 42–53.
495 <https://doi.org/10.1016/j.chroma.2017.08.023>.
- 496 [30] Q. Yu, S. Deng, G. Yu, Selective removal of perfluorooctane sulfonate from aqueous solution using chitosan-
497 based molecularly imprinted polymer adsorbents, *Water Res.* 42 (2008) 3089–3097.
498 <https://doi.org/10.1016/j.watres.2008.02.024>.
- 499 [31] D. Zou, P. Li, C. Yang, D. Han, H. Yan, Rapid determination of perfluorinated compounds in pork samples
500 using a molecularly imprinted phenolic resin adsorbent in dispersive solid phase extraction-liquid
501 chromatography tandem mass spectrometry, *Anal. Chim. Acta.* 1226 (2022) 340271-340279.
502 <https://doi.org/10.1016/j.aca.2022.340271>.
- 503 [32] J. Ren, Y. Lu, Y. Han, F. Qiao, H. Yan, Novel molecularly imprinted phenolic resin–dispersive filter extraction
504 for rapid determination of perfluorooctanoic acid and perfluorooctane sulfonate in milk, *Food Chem.* 400
505 (2023) 134062-134069. <https://doi.org/10.1016/j.foodchem.2022.134062>.
- 506 [33] C.J. Tan, Y.W. Tong, Molecularly imprinted beads by surface imprinting, *Anal. Bioanal. Chem.* 389 (2007)
507 369–376. <https://doi.org/10.1007/s00216-007-1362-4>.
- 508 [34] L. Du, Z. Cheng, P. Zhu, Q. Chen, Y. Wu, K. Tan, Preparation of mesoporous silica nanoparticles molecularly
509 imprinted polymer for efficient separation and enrichment of perfluorooctane sulfonate, *J. Sep. Sci.* 41 (2018)
510 4363–4369. <https://doi.org/10.1002/jssc.201800587>.
- 511 [35] F. Cao, L. Wang, Y. Yao, F. Wu, H. Sun, S. Lu, Synthesis and application of a highly selective molecularly
512 imprinted adsorbent based on multi-walled carbon nanotubes for selective removal of perfluorooctanoic acid,
513 *Environ. Sci. Water Res. Technol.* 4 (2018) 689–700. <https://doi.org/10.1039/C7EW00443E>.
- 514 [36] L. Du, Y. Wu, X. Zhang, F. Zhang, X. Chen, Z. Cheng, F. Wu, K. Tan, Preparation of magnetic molecularly
515 imprinted polymers for the rapid and selective separation and enrichment of perfluorooctane sulfonate, *J. Sep.*
516 *Sci.* 40 (2017) 2819–2826. <https://doi.org/10.1002/jssc.201700157>.
- 517 [37] L. Lin, H. Guo, S. Lin, Y. Chen, L. Yan, E. Zhu, K. Li, Selective extraction of perfluorooctane sulfonate in real
518 samples by superparamagnetic nanospheres coated with a polydopamine-based molecularly imprinted
519 polymer, *J. Sep. Sci.* 44 (2021) 1015–1025. <https://doi.org/10.1002/jssc.202000824>.
- 520 [38] H. Guo, Y. Liu, W. Ma, L. Yan, K. Li, S. Lin, Surface molecular imprinting on carbon microspheres for fast and
521 selective adsorption of perfluorooctane sulfonate, *J. Hazard. Mater.* 348 (2018) 29–38.
522 <https://doi.org/10.1016/j.jhazmat.2018.01.018>.

- 523 [39] L. Hu, Y. Li, W. Zhang, Characterization and application of surface-molecular-imprinted-polymer modified
524 TiO₂ nanotubes for removal of perfluorinated chemicals, *Water Sci. Technol.* 74 (2016) 1417–1425.
525 <https://doi.org/10.2166/wst.2016.321>.
- 526 [40] Y. Wu, Y. Li, A. Tian, K. Mao, J. Liu, Selective Removal of Perfluorooctanoic Acid Using Molecularly
527 Imprinted Polymer-Modified TiO₂ Nanotube Arrays, *Int. J. Photoenergy.* 2016 (2016) 1–10.
528 <https://doi.org/10.1155/2016/7368795>.
- 529 [41] K.-U. Goss, The p*K*_a Values of PFOA and Other Highly Fluorinated Carboxylic Acids, *Environ. Sci. Technol.*
530 42 (2008) 456–458. <https://doi.org/10.1021/es702192c>.
- 531 [42] D. Brooke, A. Footitt, T.A. Nwaogu, Great Britain, Environment Agency, Environmental risk evaluation report ;
532 Perfluorooctanesulphonate (PFOS), Environment Agency, Bristol, 2009.
- 533 [43] D. Zhang, Q. He, M. Wang, W. Zhang, Y. Liang, Sorption of perfluoroalkylated substances (PFASs) onto
534 granular activated carbon and biochar, *Environ. Technol.* 42 (2021) 1798–1809.
535 <https://doi.org/10.1080/09593330.2019.1680744>.
- 536 [44] Y. Zhi, J. Liu, Adsorption of perfluoroalkyl acids by carbonaceous adsorbents: Effect of carbon surface
537 chemistry, *Environ. Pollut.* 202 (2015) 168–176. <https://doi.org/10.1016/j.envpol.2015.03.019>.
- 538 [45] Y. Qu, C. Zhang, F. Li, X. Bo, G. Liu, Q. Zhou, Equilibrium and kinetics study on the adsorption of
539 perfluorooctanoic acid from aqueous solution onto powdered activated carbon, *J. Hazard. Mater.* 169 (2009)
540 146–152. <https://doi.org/10.1016/j.jhazmat.2009.03.063>.
- 541 [46] J. Li, Q. Li, L. Li, L. Xu, Removal of perfluorooctanoic acid from water with economical mesoporous
542 melamine-formaldehyde resin microsphere, *Chem. Eng. J.* 320 (2017) 501–509.
543 <https://doi.org/10.1016/j.cej.2017.03.073>.
- 544 [47] Y. Gao, S. Deng, Z. Du, K. Liu, G. Yu, Adsorptive removal of emerging polyfluoroalkyl substances F-53B and
545 PFOS by anion-exchange resin: A comparative study, *J. Hazard. Mater.* 323 (2017) 550–557.
546 <https://doi.org/10.1016/j.jhazmat.2016.04.069>.
- 547 [48] L. Zhao, J. Bian, Y. Zhang, L. Zhu, Z. Liu, Comparison of the sorption behaviors and mechanisms of
548 perfluorosulfonates and perfluorocarboxylic acids on three kinds of clay minerals, *Chemosphere.* 114 (2014)
549 51–58. <https://doi.org/10.1016/j.chemosphere.2014.03.098>.
- 550 [49] M. Mehmaddoust, N. Erk, C. Karaman, O. Karaman, An electrochemical molecularly imprinted sensor based
551 on CuBi₂O₄/rGO@MoS₂ nanocomposite and its utilization for highly selective and sensitive for linagliptin
552 assay, *Chemosphere.* 291 (2022) 132807-132817. <https://doi.org/10.1016/j.chemosphere.2021.132807>.
- 553 [50] Z. Du, S. Deng, S. Zhang, B. Wang, J. Huang, Y. Wang, G. Yu, B. Xing, Selective and High Sorption of
554 Perfluorooctanesulfonate and Perfluorooctanoate by Fluorinated Alkyl Chain Modified Montmorillonite, *J.*
555 *Phys. Chem. C.* 120 (2016) 16782–16790. <https://doi.org/10.1021/acs.jpcc.6b04757>.
- 556 [51] Y. Zhou, Z. He, Y. Tao, Y. Xiao, T. Zhou, T. Jing, Y. Zhou, S. Mei, Preparation of a functional silica membrane
557 coated on Fe₃O₄ nanoparticle for rapid and selective removal of perfluorinated compounds from surface water
558 sample, *Chem. Eng. J.* 303 (2016) 156–166. <https://doi.org/10.1016/j.cej.2016.05.137>.
- 559 [52] Md. Al Amin, Z. Sobhani, S. Chadalavada, R. Naidu, C. Fang, Smartphone-based / Fluoro-SPE for selective
560 detection of PFAS at ppb level, *Environ. Technol. Innov.* 18 (2020) 100778-100785.
561 <https://doi.org/10.1016/j.eti.2020.100778>.
- 562 [53] M. Al Amin, Y. Luo, A. Nolan, F. Robinson, J. Niu, S. Warner, Y. Liu, R. Dharmarajan, M. Mallavarapu, R.
563 Naidu, C. Fang, Total oxidisable precursor assay towards selective detection of PFAS in AFFF, 2021.
- 564 [54] R.B. Clark, J.E. Dick, Towards deployable electrochemical sensors for per- and polyfluoroalkyl substances
565 (PFAS), *Chem. Commun.* 57 (2021) 8121–8130. <https://doi.org/10.1039/D1CC02641K>.
- 566 [55] D. Grieshaber, R. MacKenzie, J. Voros, E. Reimhult, *Electrochemical Biosensors - Sensor Principles and*
567 *Architectures*, (2008) 59.
- 568 [56] B. Mostafiz, S.A. Bigdeli, K. Banan, H. Afsharara, D. Hatamabadi, P. Mousavi, C.M. Hussain, R. Keçili, F.
569 Ghorbani-Bidkorbeh, Molecularly imprinted polymer-carbon paste electrode (MIP-CPE)-based sensors for the
570 sensitive detection of organic and inorganic environmental pollutants: A review, *Trends Environ. Anal. Chem.*
571 32 (2021) e00144-e00144. <https://doi.org/10.1016/j.teac.2021.e00144>.

- 572 [57] Y. Pan, D. Shan, L. Ding, X. Yang, K. Xu, H. Huang, J. Wang, H. Ren, Developing a generally applicable
573 electrochemical sensor for detecting macrolides in water with thiophene-based molecularly imprinted
574 polymers, *Water Res.* 205 (2021) 117670-117678. <https://doi.org/10.1016/j.watres.2021.117670>.
- 575 [58] C. Unger, P.A. Lieberzeit, Molecularly imprinted thin film surfaces in sensing: Chances and challenges, *React.*
576 *Funct. Polym.* 161 (2021) 104855-104864. <https://doi.org/10.1016/j.reactfunctpolym.2021.104855>.
- 577 [59] Y. Zhang, Z. Liu, Y. Wang, X. Kuang, H. Ma, Q. Wei, Directly assembled electrochemical sensor by combining
578 self-supported CoN nanoarray platform grown on carbon cloth with molecularly imprinted polymers for the
579 detection of Tylosin, *J. Hazard. Mater.* 398 (2020) 122778-122786.
580 <https://doi.org/10.1016/j.jhazmat.2020.122778>.
- 581 [60] R. Crapnell, A. Hudson, C. Foster, K. Eersels, B. Grinsven, T. Cleij, C. Banks, M. Peeters, Recent Advances in
582 Electrosynthesized Molecularly Imprinted Polymer Sensing Platforms for Bioanalyte Detection, *Sensors.* 19
583 (2019) 1204-1231. <https://doi.org/10.3390/s19051204>.
- 584 [61] C. Malitesta, I. Losito, P.G. Zambonin, Molecularly Imprinted Electrosynthesized Polymers: New Materials for
585 Biomimetic Sensors, *Anal. Chem.* 71 (1999) 1366-1370. <https://doi.org/10.1021/ac980674g>.
- 586 [62] C. Malitesta, E. Mazzotta, R.A. Picca, A. Poma, I. Chianella, S.A. Piletsky, MIP sensors – the electrochemical
587 approach, *Anal. Bioanal. Chem.* 402 (2012) 1827-1846. <https://doi.org/10.1007/s00216-011-5405-5>.
- 588 [63] R. Kazemi, E.I. Potts, J.E. Dick, Quantifying Interferent Effects on Molecularly Imprinted Polymer Sensors for
589 Per- and Polyfluoroalkyl Substances (PFAS), *Anal. Chem.* 92 (2020) 10597-10605.
590 <https://doi.org/10.1021/acs.analchem.0c01565>.
- 591 [64] D. Lu, D.Z. Zhu, H. Gan, Z. Yao, J. Luo, S. Yu, P. Kurup, An ultra-sensitive molecularly imprinted polymer
592 (MIP) and gold nanostars (AuNS) modified voltammetric sensor for facile detection of perfluorooctane
593 sulfonate (PFOS) in drinking water, *Sens. Actuators B Chem.* 352 (2022) 131055-131065.
594 <https://doi.org/10.1016/j.snb.2021.131055>.
- 595 [65] N. Karimian, A.M. Stortini, L.M. Moretto, C. Costantino, S. Bogialli, P. Ugo, Electrochemosensor for Trace
596 Analysis of Perfluorooctanesulfonate in Water Based on a Molecularly Imprinted Poly(*o*-phenylenediamine)
597 Polymer, *ACS Sens.* 3 (2018) 1291-1298. <https://doi.org/10.1021/acssensors.8b00154>.
- 598 [66] G. Moro, D. Cristofori, F. Bottari, E. Cattaruzza, K. De Wael, L.M. Moretto, Redesigning an Electrochemical
599 MIP Sensor for PFOS: Practicalities and Pitfalls, *Sensors.* 19 (2019) 4433-4445.
600 <https://doi.org/10.3390/s19204433>.
- 601 [67] J. Luo, J. Huang, Y. Wu, J. Sun, W. Wei, X. Liu, Synthesis of hydrophilic and conductive molecularly imprinted
602 polyaniline particles for the sensitive and selective protein detection, *Biosens. Bioelectron.* 94 (2017) 39-46.
603 <https://doi.org/10.1016/j.bios.2017.02.035>.
- 604 [68] A. Kausaite-Minkstimiene, V. Mazeiko, A. Ramanaviciene, A. Ramanavicius, Enzymatically synthesized
605 polyaniline layer for extension of linear detection region of amperometric glucose biosensor, *Biosens.*
606 *Bioelectron.* 26 (2010) 790-797. <https://doi.org/10.1016/j.bios.2010.06.023>.
- 607 [69] L. Özcan, M. Sahin, Y. Sahin, Electrochemical Preparation of a Molecularly Imprinted Polypyrrole-modified
608 Pencil Graphite Electrode for Determination of Ascorbic Acid, *Sensors (Basel)* 8 (2008) 5792-5805.
609 <https://doi.org/10.3390/s8095792>
- 610 [70] A.A. Wani, A. M. Khan, Y. K. Manea, M. A.S. Salem, M. Shahadat, Selective adsorption and ultrafast
611 fluorescent detection of Cr(VI) in wastewater using neodymium doped polyaniline supported layered double
612 hydroxide nanocomposite, *J. Hazard. Mater.* 416 (2021) 125754-125765.
613 <https://doi.org/10.1016/j.jhazmat.2021.125754>.
- 614 [71] T.-Y. Chi, Z. Chen, J. Kameoka, Perfluorooctanesulfonic Acid Detection Using Molecularly Imprinted
615 Polyaniline on a Paper Substrate, *Sensors.* 20 (2020) 7301-7315. <https://doi.org/10.3390/s20247301>.
- 616 [72] C. Fang, Z. Chen, M. Megharaj, R. Naidu, Potentiometric detection of AFFFs based on MIP, *Environ. Technol.*
617 *Innov.* 5 (2016) 52-59. <https://doi.org/10.1016/j.eti.2015.12.003>.
- 618 [73] J. Gong, T. Fang, D. Peng, A. Li, L. Zhang, A highly sensitive photoelectrochemical detection of
619 perfluorooctanic acid with molecularly imprinted polymer-functionalized nanoarchitected hybrid of AgI-
620 BiOI composite, *Biosens. Bioelectron.* 73 (2015) 256-263. <https://doi.org/10.1016/j.bios.2015.06.008>.

- 621 [74] X. Li, X. Wang, T. Fang, L. Zhang, J. Gong, Disposable photoelectrochemical sensing strip for highly sensitive
622 determination of perfluorooctane sulfonyl fluoride on functionalized screen-printed carbon electrode, *Talanta*.
623 181 (2018) 147–153. <https://doi.org/10.1016/j.talanta.2018.01.005>.
- 624 [75] T. Tran, T. J. Li, H. Feng, J. Cai, L. Yuan, N. Wang, Q. Cai, Molecularly imprinted polymer modified TiO₂
625 nanotube arrays for photoelectrochemical determination of perfluorooctane sulfonate (PFOS), *Sens. Actuators*
626 *B Chem.* 190 (2014) 745–751. <https://doi.org/10.1016/j.snb.2013.09.048>.
- 627 [76] S. Chen, A. Li, L. Zhang, J. Gong, Molecularly imprinted ultrathin graphitic carbon nitride nanosheets–Based
628 electrochemiluminescence sensing probe for sensitive detection of perfluorooctanoic acid, *Anal. Chim. Acta*.
629 896 (2015) 68–77. <https://doi.org/10.1016/j.aca.2015.09.022>.
- 630 [77] H. Feng, N. Wang, T. Tran, T. L. Yuan, J. Li, Q. Cai, Surface molecular imprinting on dye–(NH₂)–SiO₂ NPs for
631 specific recognition and direct fluorescent quantification of perfluorooctane sulfonate, *Sens. Actuators B Chem.*
632 195 (2014) 266–273. <https://doi.org/10.1016/j.snb.2014.01.036>.
- 633 [78] Z. Jiao, J. Li, L. Mo, J. Liang, H. Fan, A molecularly imprinted chitosan doped with carbon quantum dots for
634 fluorometric determination of perfluorooctane sulfonate, *Microchim. Acta.* 185 (2018) 473–481.
635 <https://doi.org/10.1007/s00604-018-2996-y>.
- 636 [79] L. Zheng, Y. Zheng, Y. Liu, S. Long, L. Du, J. Liang, C. Huang, M.T. Swihart, K. Tan, Core-shell quantum dots
637 coated with molecularly imprinted polymer for selective photoluminescence sensing of perfluorooctanoic acid,
638 *Talanta*. 194 (2019) 1–6. <https://doi.org/10.1016/j.talanta.2018.09.106>.
- 639 [80] N. Cennamo, G. D’Agostino, G. Porto, A. Biasiolo, C. Perri, F. Arcadio, L. Zeni, A Molecularly Imprinted
640 Polymer on a Plasmonic Plastic Optical Fiber to Detect Perfluorinated Compounds in Water, *Sensors*. 18
641 (2018) 1836–1846. <https://doi.org/10.3390/s18061836>.
- 642 [81] W.-W. Zhao, M. Xiong, X.-R. Li, J.-J. Xu, H.-Y. Chen, Photoelectrochemical bioanalysis: A mini review,
643 *Electrochem. Commun.* 38 (2014) 40–43. <https://doi.org/10.1016/j.elecom.2013.10.035>.
- 644 [82] W.-W. Zhao, J.-J. Xu, H.-Y. Chen, Photoelectrochemical bioanalysis: the state of the art, *Chem. Soc. Rev.* 44
645 (2015) 729–741. <https://doi.org/10.1039/C4CS00228H>.
- 646 [83] L. Shi, Y. Yin, L.-C. Zhang, S. Wang, M. Sillanpää, H. Sun, Design and engineering heterojunctions for the
647 photoelectrochemical monitoring of environmental pollutants: A review, *Appl. Catal. B Environ.* 248 (2019)
648 405–422. <https://doi.org/10.1016/j.apcatb.2019.02.044>.
- 649 [84] K. Fährnich, M. Pravda, G. G. Guilbault, Recent applications of electrogenerated chemiluminescence in
650 chemical analysis, *Talanta*. 54 (2001) 531–559. [https://doi.org/10.1016/S0039-9140\(01\)00312-5](https://doi.org/10.1016/S0039-9140(01)00312-5).
- 651 [85] L. Hu, G. Xu, Applications and trends in electrochemiluminescence, *Chem. Soc. Rev.* 39 (2010) 3275–3304.
652 <https://doi.org/10.1039/b923679c>.
- 653 [86] L. Cumba, Y. Pellegrin, F. Melinato, R.J. Forster, Enhanced Electrochemiluminescence from 3D Nanocavity
654 Electrode Arrays, *Sens. Actuators Rep.* 4 (2022) 100082–100087. <https://doi.org/10.1016/j.snr.2022.100082>.
- 655 [87] N.P. Sardesai, J.C. Barron, J.F. Rusling, Carbon Nanotube Microwell Array for Sensitive
656 Electrochemiluminescent Detection of Cancer Biomarker Proteins, *Anal. Chem.* 83 (2011) 6698–6703.
657 <https://doi.org/10.1021/ac201292q>.
- 658 [88] H. Yu, J.G. Bruno, Immunomagnetic–electrochemiluminescent detection of *Escherichia coli* O157 and
659 *Salmonella typhimurium* in foods and environmental water samples, *Appl. Environ. Microbiol.* 62 (1996)
660 587–592. <https://doi.org/10.1128/aem.62.2.587-592.1996>.
- 661 [89] G. Jie, L. Li, C. Chen, J. Xuan, J.-J. Zhu, Enhanced electrochemiluminescence of CdSe quantum dots
662 composited with CNTs and PDDA for sensitive immunoassay, *Biosens. Bioelectron.* 24 (2009) 3352–3358.
663 <https://doi.org/10.1016/j.bios.2009.04.039>.
- 664 [90] P. Rebelo, E. Costa-Rama, I. Seguro, J.G. Pacheco, H.P.A. Nouws, M.N.D.S. Cordeiro, C. Delerue-Matos,
665 Molecularly imprinted polymer-based electrochemical sensors for environmental analysis, *Biosens.*
666 *Bioelectron.* 172 (2021) 112719–112736. <https://doi.org/10.1016/j.bios.2020.112719>.
- 667 [91] K. Risha, J. Flaherty, R. Wille, W. Buck, F. Morandi, T. Isemura, Method for Trace Level Analysis of C₈, C₉,
668 C₁₀, C₁₁, and C₁₃ Perfluorocarbon Carboxylic Acids in Water, *Anal. Chem.* 77 (2005) 1503–1508.
669 <https://doi.org/10.1021/ac0490548>.

- 670 [92] C. Capolungo, D. Genovese, M. Montalti, E. Rampazzo, N. Zaccheroni, L. Prodi, Photoluminescence-Based
671 Techniques for the Detection of Micro- and Nanoplastics, *Chem. – Eur. J.* 27 (2021) 17529–17541.
672 <https://doi.org/10.1002/chem.202102692>.
- 673 [93] D.T. McQuade, A.E. Pullen, T.M. Swager, Conjugated Polymer-Based Chemical Sensors, *Chem. Rev.* 100
674 (2000) 2537–2574. <https://doi.org/10.1021/cr9801014>.
- 675 [94] X. Sun, Y. Lei, Fluorescent carbon dots and their sensing applications, *TrAC Trends Anal. Chem.* 89 (2017)
676 163–180. <https://doi.org/10.1016/j.trac.2017.02.001>.
- 677 [95] B. Qu, J. Sun, P. Li, L. Jing, Current advances on g-C₃N₄-based fluorescence detection for environmental
678 contaminants, *J. Hazard. Mater.* 425 (2022) 127990-128007. <https://doi.org/10.1016/j.jhazmat.2021.127990>.
- 679 [96] R. Gui, H. Jin, Recent advances in synthetic methods and applications of photo-luminescent molecularly
680 imprinted polymers, *J. Photochem. Photobiol. C Photochem. Rev.* 41 (2019) 100315-100352.
681 <https://doi.org/10.1016/j.jphotochemrev.2019.08.002>.
- 682 [97] V. Hodnik, G. Anderluh, Toxin Detection by Surface Plasmon Resonance, *Sensors.* 9 (2009) 1339–1354.
683 <https://doi.org/10.3390/s9031339>.
- 684 [98] Y. Wang, T.-X. Wei, Surface plasmon resonance sensor chips for the recognition of bovine serum albumin via
685 electropolymerized molecularly imprinted polymers, *Chin. Chem. Lett.* 24 (2013) 813–816.
686 <https://doi.org/10.1016/j.ccllet.2013.05.004>.
- 687 [99] Y. Saylan, A. Denizli, Molecular Fingerprints of Hemoglobin on a Nanofilm Chip, *Sensors.* 18 (2018) 3016-
688 3028. <https://doi.org/10.3390/s18093016>.
- 689 [100] G. Ertürk, H. Özen, M.A. Tümer, B. Mattiasson, A. Denizli, Microcontact imprinting based surface plasmon
690 resonance (SPR) biosensor for real-time and ultrasensitive detection of prostate specific antigen (PSA) from
691 clinical samples, *Sens. Actuators B Chem.* 224 (2016) 823–832. <https://doi.org/10.1016/j.snb.2015.10.093>.
- 692 [101] R. Verma, B.D. Gupta, Optical fiber sensor for the detection of tetracycline using surface plasmon resonance and
693 molecular imprinting, *The Analyst.* 138 (2013) 7254–7263. <https://doi.org/10.1039/c3an01098h>.
- 694 [102] N. Cennamo, G. D'Agostino, R. Galatus, L. Bibbò, M. Pesavento, L. Zeni, Sensors based on surface plasmon
695 resonance in a plastic optical fiber for the detection of trinitrotoluene, *Sens. Actuators B Chem.* 188 (2013)
696 221–226. <https://doi.org/10.1016/j.snb.2013.07.005>.
- 697 [103] H. Agrawal, A.M. Shrivastav, B.D. Gupta, Surface plasmon resonance based optical fiber sensor for atrazine
698 detection using molecular imprinting technique, *Sens. Actuators B Chem.* 227 (2016) 204–211.
699 <https://doi.org/10.1016/j.snb.2015.12.047>.
- 700 [104] A.M. Shrivastav, S.P. Usha, B.D. Gupta, Fiber optic profenofos sensor based on surface plasmon resonance
701 technique and molecular imprinting, *Biosens. Bioelectron.* 79 (2016) 150–157.
702 <https://doi.org/10.1016/j.bios.2015.11.095>.
- 703 [105] N. Cennamo, L. Zeni, P. Tortora, M.E. Regonesi, A. Giusti, M. Staiano, S. D'Auria, A. Varriale, A High
704 Sensitivity Biosensor to detect the presence of perfluorinated compounds in environment, *Talanta.* 178 (2018)
705 955–961. <https://doi.org/10.1016/j.talanta.2017.10.034>.
- 706 [106] N. Cennamo, G. D'Agostino, F. Sequeira, F. Mattiello, G. Porto, A. Biasiolo, R. Nogueira, L. Bilro, L. Zeni, A
707 Simple and Low-Cost Optical Fiber Intensity-Based Configuration for Perfluorinated Compounds in Water
708 Solution, *Sensors.* 18 (2018) 3009-3019. <https://doi.org/10.3390/s18093009>.
- 709